

CRITICAL METALS IN LATERITE RELATED TO PEGMATITE MINERAL SYSTEMS OF THE WESTERN YILGARN CRATON (Li, W, Sn, Ta, REE)

A Otto, H Lampinen, T Pinchand, J Huntington and R Noble





Government of **Western Australia**
Department of **Mines, Industry Regulation
and Safety**

REPORT 233

CRITICAL METALS IN LATERITE RELATED TO PEGMATITE MINERAL SYSTEMS OF THE WESTERN YILGARN CRATON (Li, W, Sn, Ta, REE)

A Otto, H Lampinen, T Pinchand, J Huntington and R Noble

PERTH 2022



**Geological Survey of
Western Australia**

MINISTER FOR MINES AND PETROLEUM
Hon Bill Johnston MLA

DIRECTOR GENERAL, DEPARTMENT OF MINES, INDUSTRY REGULATION AND SAFETY
Richard Sellers

EXECUTIVE DIRECTOR, GEOLOGICAL SURVEY AND RESOURCE STRATEGY
Jeff Haworth

REFERENCE

The recommended reference for this publication is:

Otto A, Lampinen H, Pinchand T, Huntington, J and Noble, R 2022, Critical metals in laterite related to pegmatite mineral systems of the western Yilgarn Craton (Li, W, Sn, Ta, REE): Geological Survey of Western Australia, Report 233, 43p.

ISBN 978-1-74168-974-7

ISSN 1834-2280



A catalogue record for this book is available from the National Library of Australia



About this publication

This Report was prepared by the Commonwealth Scientific and Industrial Research Organisation (CSIRO), and commissioned by the Geological Survey of Western Australia (GSWA). GSWA is releasing the information as part of its Report Series to ensure a wider distribution of the results. Although GSWA provided support to the project, the scientific content of the Report, and the drafting of figures, has been the responsibility of CSIRO. No editing has been undertaken by GSWA.

Disclaimer

This product uses information from various sources. The Department of Mines, Industry Regulation and Safety (DMIRS) and the State cannot guarantee the accuracy, currency or completeness of the information. Neither the department nor the State of Western Australia nor any employee or agent of the department shall be responsible or liable for any loss, damage or injury arising from the use of or reliance on any information, data or advice (including incomplete, out of date, incorrect, inaccurate or misleading information, data or advice) expressed or implied in, or coming from, this publication or incorporated into it by reference, by any person whatsoever.

Published 2022 by the Geological Survey of Western Australia

This Report is published in digital format (PDF) and is available online at <www.dmirs.wa.gov.au/GSWApublications>.



© State of Western Australia (Department of Mines, Industry Regulation and Safety) 2022

With the exception of the Western Australian Coat of Arms and other logos, and where otherwise noted, these data are provided under a Creative Commons Attribution 4.0 International Licence. (<https://creativecommons.org/licenses/by/4.0/legalcode>)

Further details of geoscience products are available from:

First Floor Counter
Department of Mines, Industry Regulation and Safety
100 Plain Street
EAST PERTH WESTERN AUSTRALIA 6004
Telephone: +61 8 9222 3459 Email: publications@dmirs.wa.gov.au
www.dmirs.wa.gov.au/GSWApublications

Cover photograph: Example spatial plots of new geochemical data sourced from laterite samples in the western Yilgarn Craton



Australia's National
Science Agency

Critical metals in laterite related to pegmatite mineral systems of the western Yilgarn Craton (Li, W, Sn, Ta, REE)

EP 2021-3481 Final Report, April 2022

Authors: Alexander Otto, Heta Lampinen, Tenten Pinchand, Jon Huntington, Ryan Noble

Citation

Otto A., Lampinen H., Pinchand T., Huntington J., Noble, R., 2022. Critical metals in laterite related to pegmatite mineral systems of the western Yilgarn Craton (Li, W, Sn, Ta, REE). EP 2021-3481, CSIRO, Australia. p.43

Copyright

© Commonwealth Scientific and Industrial Research Organisation 2020. To the extent permitted by law, all rights are reserved and no part of this publication covered by copyright may be reproduced or copied in any form or by any means except with the written permission of CSIRO.

Important disclaimer

CSIRO advises that the information contained in this publication comprises general statements based on scientific research. The reader is advised and needs to be aware that such information may be incomplete or unable to be used in any specific situation. No reliance or actions must therefore be made on that information without seeking prior expert professional, scientific and technical advice. To the extent permitted by law, CSIRO (including its employees and consultants) excludes all liability to any person for any consequences, including but not limited to all losses, damages, costs, expenses and any other compensation, arising directly or indirectly from using this publication (in part or in whole) and any information or material contained in it.

CSIRO is committed to providing web accessible content wherever possible. If you are having difficulties with accessing this document, please contact csiroenquiries@csiro.au.

Contents

Acknowledgments.....	v
Executive summary	vi
1 Introduction	1
1.1 Digital data record	2
2 Sample preparation and analytical methods.....	3
2.1 Sample handling and certified reference material.....	3
2.2 Sample preparation	3
2.3 Mineralogical Methods	3
3 Results.....	6
3.1 Geochemistry	6
3.2 Mineralogy.....	33
4 Discussion and Future.....	41
5 References	43

Figures

Figure 1 Lithium values for OREAS 20a certified reference material with lower and upper two standard deviation.	7
Figure 2 Lithium values for OREAS 45f certified reference material with lower and upper two standard deviation.	7
Figure 3 Platinum values for OREAS 45f certified reference material with lower and upper two standard deviation.	7
Figure 4 Platinum values for 58 samples analysed with fire assay ICP-MS (Pt_ppb_FA_new) versus multi-acid digest ICP-MS (Pt_ppb_new).	8
Figure 5 Diagram showing the values for the new versus original analysis for barium, demonstrating the improved precision through a lower detection limit.	8
Figure 6 Diagram showing the values for the original versus new analysis for zirconium, showing large discrepancy due to different digest methods (fusion vs multi-acid digest).	9
Figure 7 Barium distribution in the SW Yilgarn with 500K interpreted geology.	11
Figure 8 Beryllium distribution in the SW Yilgarn with 500K interpreted geology.	12
Figure 9 Caesium distribution in the SW Yilgarn with 500K interpreted geology.	13
Figure 10 Chromium distribution in the SW Yilgarn with 500K interpreted geology.	14
Figure 11 Cobalt distribution in the SW Yilgarn with 500K interpreted geology.	15
Figure 12 Dysprosium distribution in the SW Yilgarn with 500K interpreted geology.	16
Figure 13 Hafnium distribution in the SW Yilgarn with 500K interpreted geology.	17
Figure 14 Holmium distribution in the SW Yilgarn with 500K interpreted geology.	18
Figure 15 Lithium distribution in the SW Yilgarn with 500K interpreted geology.	19
Figure 16 Mercury distribution in the SW Yilgarn with 500K interpreted geology.	20
Figure 17 Niobium distribution in the SW Yilgarn with 500K interpreted geology.	21
Figure 18 Platinum distribution in the SW Yilgarn with 500K interpreted geology.	22
Figure 19 Rhenium distribution in the SW Yilgarn with 500K interpreted geology.	23
Figure 20 Rubidium distribution in the SW Yilgarn with 500K interpreted geology.	24
Figure 21 Scandium distribution in the SW Yilgarn with 500K interpreted geology.	25
Figure 22 Silver distribution in the SW Yilgarn with 500K interpreted geology.	26
Figure 23 Tantalum distribution in the SW Yilgarn with 500K interpreted geology.	27
Figure 24 Thorium distribution in the SW Yilgarn with 500K interpreted geology.	28
Figure 25 Tin distribution in the SW Yilgarn with 500K interpreted geology.	29
Figure 26 Tungsten distribution in the SW Yilgarn with 500K interpreted geology.	30
Figure 27 Uranium distribution in the SW Yilgarn with 500K interpreted geology.	31

Figure 28 Zirconium distribution in the SW Yilgarn with 500K interpreted geology.....	32
Figure 29. Kaolinite relative abundance (qualitative weight in TSA output of identified phases only) delineated from HyLogger-3™ data indicating significant spatial difference in the mineralogic composition of the laterite samples between southwest and northeast of the sampled area of the Yilgarn Craton.	34
Figure 30. Gibbsite relative abundance (qualitative weight in TSA output of identified phases only) delineated from HyLogger-3™ data indicating significant spatial difference in the mineralogic composition of the laterite samples between southwest and northeast of the sampled area of the Yilgarn Craton	35
Figure 31. Goethite relative abundance (qualitative weight in TSA output of identified phases only) delineated from HyLogger-3 data indicating significant spatial difference in the mineralogic composition of the laterite samples between southwest and northeast of the sampled area of the Yilgarn Craton.	36
Figure 32. XRD spectra with goethite as the main iron phase.....	37
Figure 33 XRD spectra with hematite as the main iron phase.	38
Figure 34. XRD spectra with all aluminium phases present, kaolinite, gibbsite, boehmite.	38
Figure 35 Image of bright-phase mapping particles.	40

Tables

Table 1 Details of analytical investigations.	1
Table 2 Univariate statistics for new data of samples that have results above detection limit. Units are ppm except for Pt in ppb, bdl = below detection limit.	10
Table 3 Quantitative (vol%) results from bright-phase mapping of pulps from 5 laterite samples.	39

Digital Data

Geochemistry:

SW Yilgarn Laterite 2020 Critical Metals.xlsx

SW Yilgarn Laterite QAQC updated April 2022.xlsx

HyLogger:

SW Yilgarn Laterite 2020 HyLogger spectral data.zip

Mineralogy:

SW Yilgarn Laterite 2020 XRD data.zip

SW Yilgarn Laterite 2020 trace mineralogy.zip

Acknowledgments

The Geological Survey of Western Australia (GSWA) is thanked for providing financial and logistical support. Jack Lowrey (GSWA) is thanked for his assistance with geochemical data quality assurance and quality control.

Monica LeGras, Mike Verrall, Derek Winchester at CSIRO Mineral Resources are thanked for their contribution and discussion.

Executive summary

This project achieved significant value addition to the ca. 20-year-old collection of laterite samples from the southwest Yilgarn craton. The analytical range has been extended to elements including lithium and platinum. Several elements such as barium, tantalum and tin were reanalysed to achieve much lower detection limits resulting in more precise definition in samples with low abundance. An addition to the dataset are NIR, SWIR and thermal spectral data for most of the samples, collected by a HyLogger-3TM system. Preliminary interpretation shows significant spatial differences in the mineralogy of the samples on the regional scale. X-ray diffraction analyses were conducted to support the initial interpretation of the spectral mineralogy data. Exploratory analysis of the trace mineralogy of these laterite samples indicates there is potential value in further assessment of the trace mineral phases for exploration. The addition of the HyLogger-3TM spectral data showed major landscape changes in the general mineralogy of the laterite with shifts from a dominance of kaolinite in the NE trending to a dominance of gibbsite in the SW. The possibility to utilise laterite mineral changes such as kaolinite crystallinity and iron oxide composition to improve trace element targeting for mineral exploration purposes exists. This warrants further study that is now possible with this expanded data resource for Western Australia.

1 Introduction

Current exploration and mining of critical metals (i.e., Li, Ta, Sn, W, REE) associated with felsic intrusive rocks (i.e., pegmatites) are focussed largely on outcropping deposits. A key challenge in the future is to understand the occurrence of deposits within pegmatite fields; the fertility of those fields at regional scale; and to discover deposits under cover.

Over several decades CSIRO has collected laterite samples in the southwestern Yilgarn Craton, which encouraged new exploration activities for gold and base metals after the data was released in the 2000's. More recently, Western Australia is becoming a hub for critical metal exploration and mining with several active projects across the Pilbara and Yilgarn cratons.

The laterite geochemistry dataset is an opportunity to provide a valuable tool to explore for these critical metals at the regional scale.

However, that dataset is missing Li and several other critical metals (i.e., Sn, W, REE) are at or below the detection limit. This project aims to reanalyse the historical samples, value-add new data types, and provide the following deliverables:

1. Analysis of historically collected laterite samples from the SW Yilgarn for Li and other critical elements.
2. Spectral mineralogy of the laterite samples using the HyLogger-3™ system.
3. Cross validation of spectral mineralogy outputs with XRD and/or SEM analysis.
4. A brief report outlining the analytical methods used and a brief interpretation of the critical metals and Li distribution on a regional scale.

Table 1 details the analytical methods employed to the laterite sample from the southwestern Yilgarn craton.

Table 1 Details of analytical investigations.

Item	Activity	Method	Product
1	Inventory and review of samples supplied and sample record	Manual checks	Excel file
2	Insertion of OREAS certified reference material 20a and 45f into the sample set (154 in total)		New certified reference material in paper bags
3	Multielement geochemistry for 2883 samples for Ag, Ba, Be, Co, Cr, Cs, Dy, Hf, Hg, Ho, Li, Nb, Pt, Rb, Re, Sc, Sn, Ta, Th, U, W, Zr	Microwave assisted multi-acid ICP-MS	Excel file
4	Fire assay for Pt, Pd, Au for 58 samples for QAQC purposes	FA-ICP-MS	Excel file
5	HyLogger spectral scans for 2750 samples	HyLogger-3™	TSG files
6	Qualitative XRD analysis for 47 samples	XRD	RAW, CPI, XPS files
7	Exploratory SEM analysis of trace mineralogy	SEM	Table and images

1.1 Digital data record

This report is accompanied with the following digital data packages:

1.1.1 Geochemistry

SW Yilgarn Laterite 2020 Critical Metals.xlsx contains the newly acquired data for Ag, Ba, Be, Co, Cr, Cs, Dy, Hf, Hg, Ho, Li, Nb, Pt, Rb, Re, Sc, Sn, Ta, Th, U, W, Zr for 2883 original samples.

SW Yilgarn Laterite QAQC Updated April 2022.xlsx contains the newly acquired data for Ag, Ba, Be, Co, Cr, Cs, Dy, Hf, Hg, Ho, Li, Nb, Pt, Rb, Re, Sc, Sn, Ta, Th, U, W, Zr for 154 certified reference material samples. This file also contains the newly acquired data for Pt, Pd, Au for 58 samples to cross check the performance of the multi-acid digest for Pt compared to fire assay.

1.1.2 HyLogger-3™

SW Yilgarn Laterite 2020 HyLogger spectral data.zip contains the spectral data for 2750 samples in the TSG file format including the chip tray images.

1.1.3 Mineralogy

SW Yilgarn Laterite 2020 XRD data.zip contains the newly acquired XRD for 47 samples.

2 Sample preparation and analytical methods

2.1 Sample handling and certified reference material

GSWA supplied 2788 pulp samples to CSIRO. Sample bags with standard material were taken out of the sample set due to missing information about origin and analytical data.

154 OREAS 20a and 45f certified reference material standards were introduced at about 1:20.

2.2 Sample preparation

Subsamples of laterite samples with sufficient material (n=2750) were transferred from sample bags into boxes labelled from 1 to 155 (box 139 missing from the batch), to slots in chip trays labelled with corresponding box numbers. Each slot was labelled with corresponding sample identifier that consists of box number and sample ID (CSIRO_No). The chip tray slots were protected by a plastic sheet during bag-to-slot transfer to minimise contamination across the slots. A small incision was made in the plastic sheet as a sample was funnelled in, and slots were subsequently covered with a second sheet of plastic for the duration of temporary storage and transport prior HyLogger-3TM data acquisition. In total, 158 trays were prepared for analysis. The tray slots were sealed with clear plastic tape layers immediately after HyLogger-3TM data acquisition and samples were submitted to the CSIRO archive.

2.3 Mineralogical Methods

2.3.1 Geochemistry

2743 samples had sufficient material for analysis and with 154 certified reference samples were submitted to LabWest Ltd. for analysis. The samples were digested using a microwave assisted method under high pressure and temperature in HF bearing acid mixture (lab code: MMA-04M). The elements Ag, Ba, Be, Co, Cr, Cs, Dy, Hf, Hg, Ho, Li, Nb, Pt, Rb, Re, Sc, Sn, Ta, Th, U, W, and Zr were determined by ICP-MS.

58 samples were analysed at the Bureau Veritas laboratories with a 40g fire assay with a determination of Pt, Pd, and Au by ICP-MS to confirm the validity of the Pt analysis in the multielement analysis.

2.3.2 Infrared Reflectance Spectroscopy

Infrared reflectance spectra were collected from laterite pulp samples (n=2750) held in chip trays using the CSIRO Drill core laboratory's HyLogger-3™ in chip sampling mode. Of these, 2638 samples have associated spatial data.

The methodology for HyLogger-3™ continuous line-scan data acquisition is described by Hancock and Huntington (2010), Hancock et al. (2013), and Schodlok et al. (2016a). The HyLogger-3™ chip mode setting collects three (3) data points from each chip slot, which are averaged to one output reflectance spectra per slot in the subsequent TSG (The Spectral Geologist) software file.

Reflectance spectra were collected over the visible-to-near-infrared (VNIR: 380–1000 nm), short-wave infrared (SWIR: 1000–2500 nm) and thermal infrared (TIR: 6000–14500 nm) wavelength ranges to determine the presence, abundance, composition, and other characteristics of a range of common rock-forming minerals. Extensive QA/QC of individual chip trays was undertaken during the scanning process to ensure high data quality.

High-resolution (0.1 mm pixel) digital colour photographs of samples were concurrently obtained using the built-in line-scan camera (Hancock and Huntington, 2010).

Raw (averaged) HyLogger-3™ spectral data are initially automatically processed using The Spectral Assistant (TSA) algorithm (Berman et al., 1999, 2011, 2017) which is built into the TSG software (Huntington et al., 1997 and Schodlok et al., 2016b). TSA models the acquired spectra using a reference library of 'typical' mineral spectra, and identifies the quality of the fit, and the proportion of the three or four mineral spectra that were used to generate the best fit model, which can be used as an estimate of their relative proportions (Huntington et al., 1997). These automated TSA mineral identifications were subsequently refined by filtering out minerals considered geologically out of context to remove obviously erroneous interpretations, and also by manually refining the TSA matching scalars (uTSAV, uTSAS and uTSAT), using additional scalars built-in to TSG.

Associated sample data were integrated with the project TSG file (See Digital Data: Laterite-SWYIG-box1-155). Associated data include: 1) CSIRO_No, sample medium and geographic coordinates.

2.3.3 X-ray diffraction Analysis

The samples were measured with a laboratory-based Bruker D4 XRD instrument with the following measurement parameters:

- Co cathode ($\lambda=1.78$ Angstrom).
- V = 40kV
- I = 40mA.
- 2Theta angle: 5 – 90 degrees

47 samples were analysed to qualitatively confirm the major mineralogy to validate the spectral mineralogy interpretation.

2.3.4 Scanning Electron Microscopy

Polished 23 mm rounds were produced from 5 pulp samples to explore the trace mineralogy of the sample material.

Bright-phase mapping was conducted using a Mira Tescan TM field emission gun (FEG) scanning electron microscope (SEM), coupled with three EDAX Energy Dispersive X-ray Spectroscopy (EDS) detectors, a backscatter electron (BSE) detector and the Tescan Integrated Mineral Analyser (TIMA) software package. The bright phase mapping setting on the SEM utilises a 25 keV, 6 nA, 26 nm electron beam and a 1-micron pixel size was chosen for analyses with a required minimum of 1000 X-ray counts per pixel.

3 Results

3.1 Geochemistry

3.1.1 Quality assurance and quality control

Most elements display good precision and accuracy. Some elements return consistently higher values than the historically reported data, including silver, mercury, chromium, and rubidium. Only scandium has issues with precision. In the case of lithium, most standard samples (20a, 45f) return values within two standard deviation (Figure 1 and Figure 2). Platinum values for the OREAS 45f standard return values within two standard deviation or very close to it (Figure 3). The comparison of a subset of samples analysed additionally by a fire assay digest indicates an overall good performance of the multi-acid digest for platinum (Figure 4). A comparison between the original analysis and from this study of barium demonstrate the gain in precision for samples with lower values, which is seen in most of the reanalysed elements (Figure 5). The exceptions are zirconium and hafnium, and Figure 6 demonstrates the divergence of values compared with the original analysis. The reason is in the different digest between the original assay (fusion) and the reanalysis (multi-acid). In general, the microwave extraction of the 4-acid digestion typically provides greater values than those reported with other labs using open block digestion for the OREAS standard values. This is because the microwave enables the extraction to be conducted at greater temperature and pressure, so it tends to be a little more aggressive, not lose volatile elements and in turn extract slightly more of the strongly resistate minerals and their associated elements like Ti and Zr.

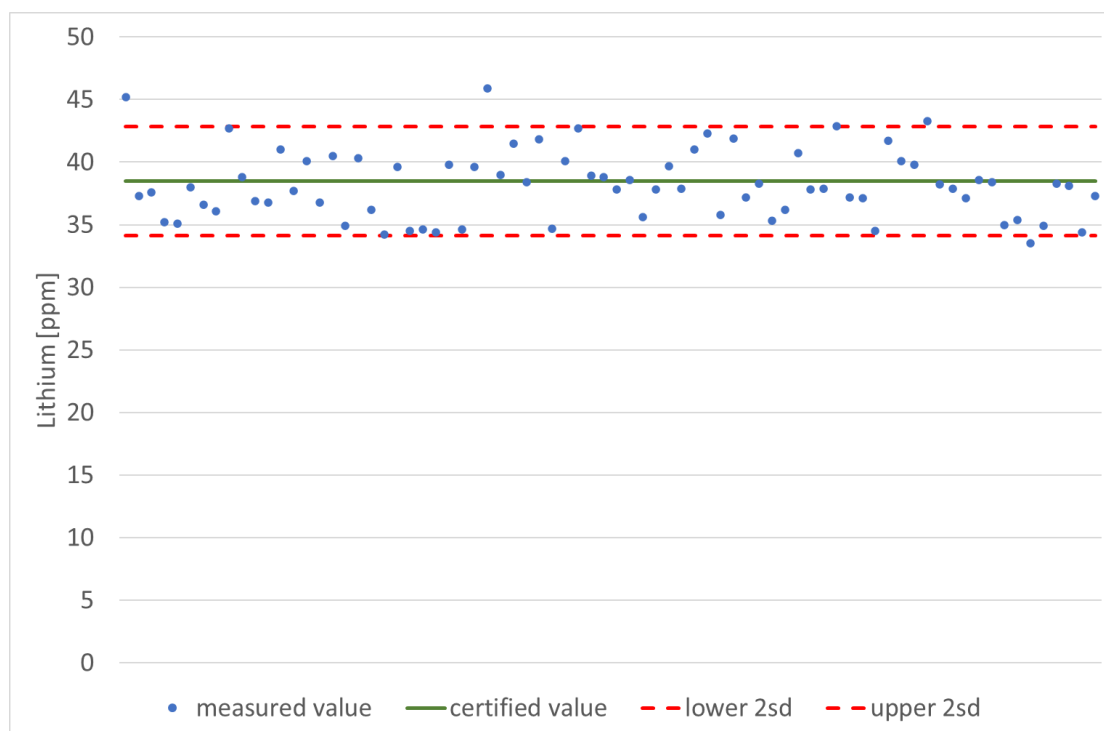


Figure 1 Lithium values for OREAS 20a certified reference material with lower and upper two standard deviation.

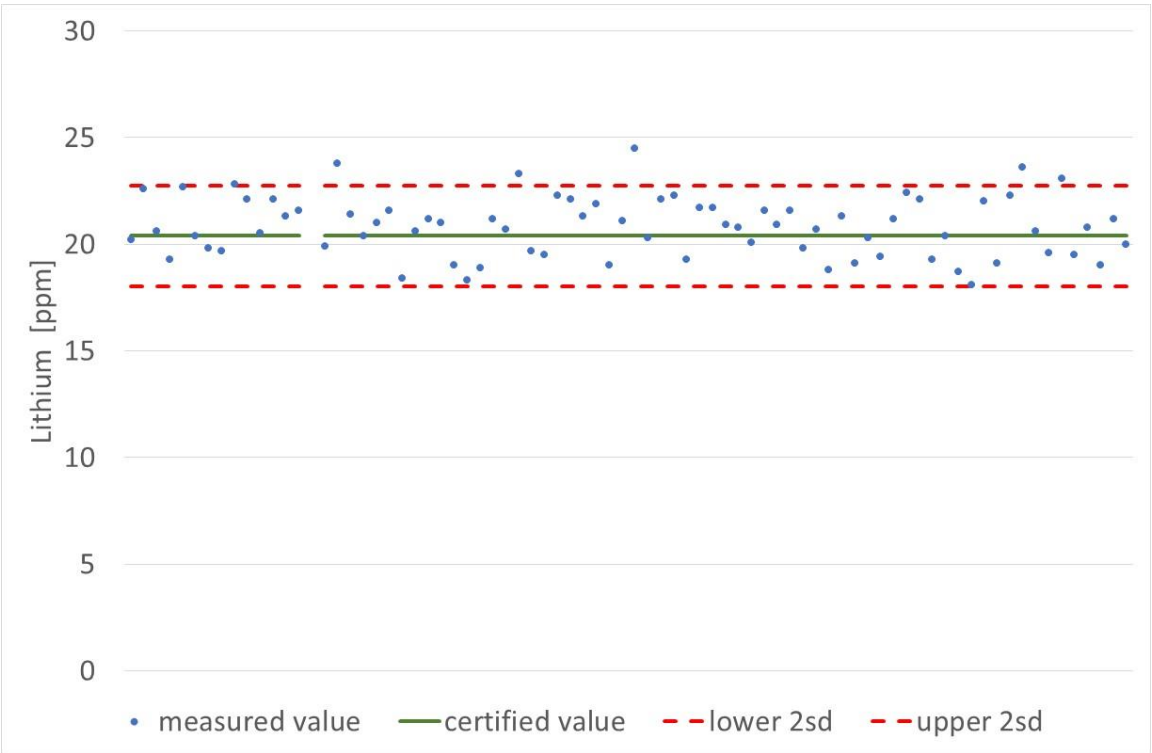


Figure 2 Lithium values for OREAS 45f certified reference material with lower and upper two standard deviation.

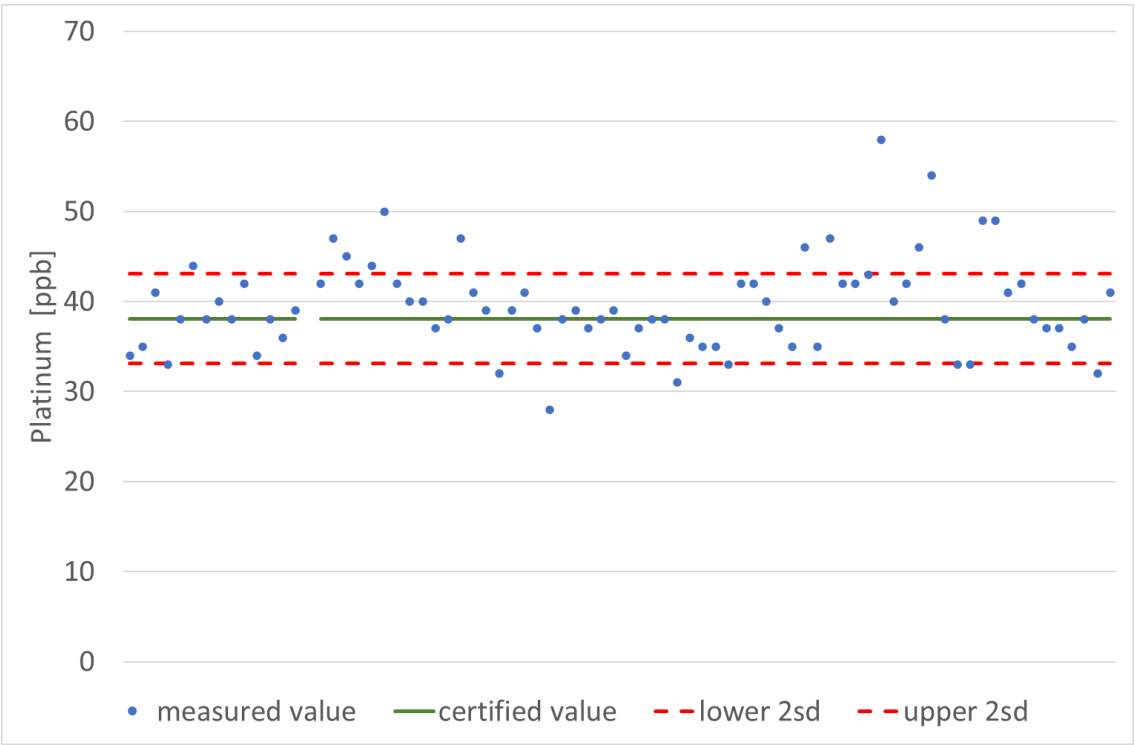


Figure 3 Platinum values for OREAS 45f certified reference material with lower and upper two standard deviation.

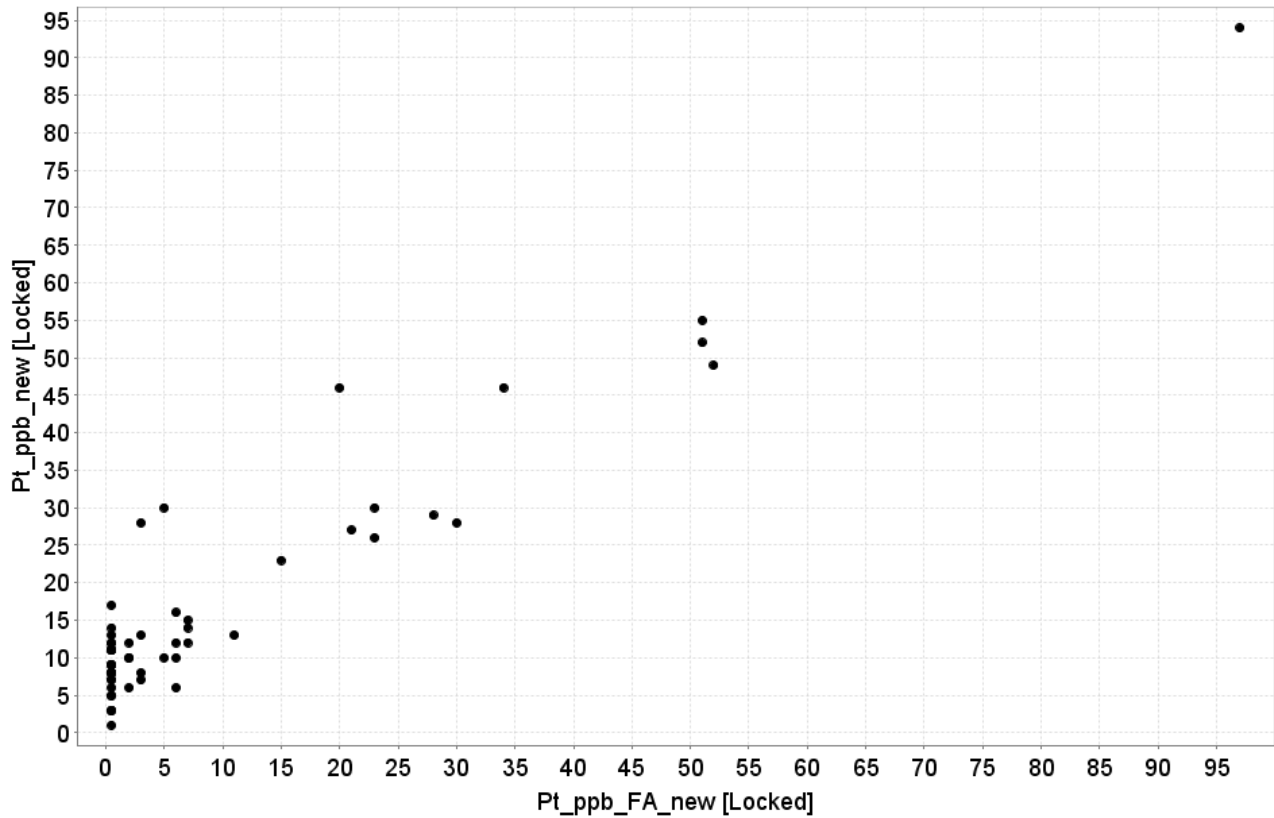


Figure 4 Platinum values for 58 samples analysed with fire assay ICP-MS (Pt_ppb_FA_new) versus multi-acid digest ICP-MS (Pt_ppb_new).

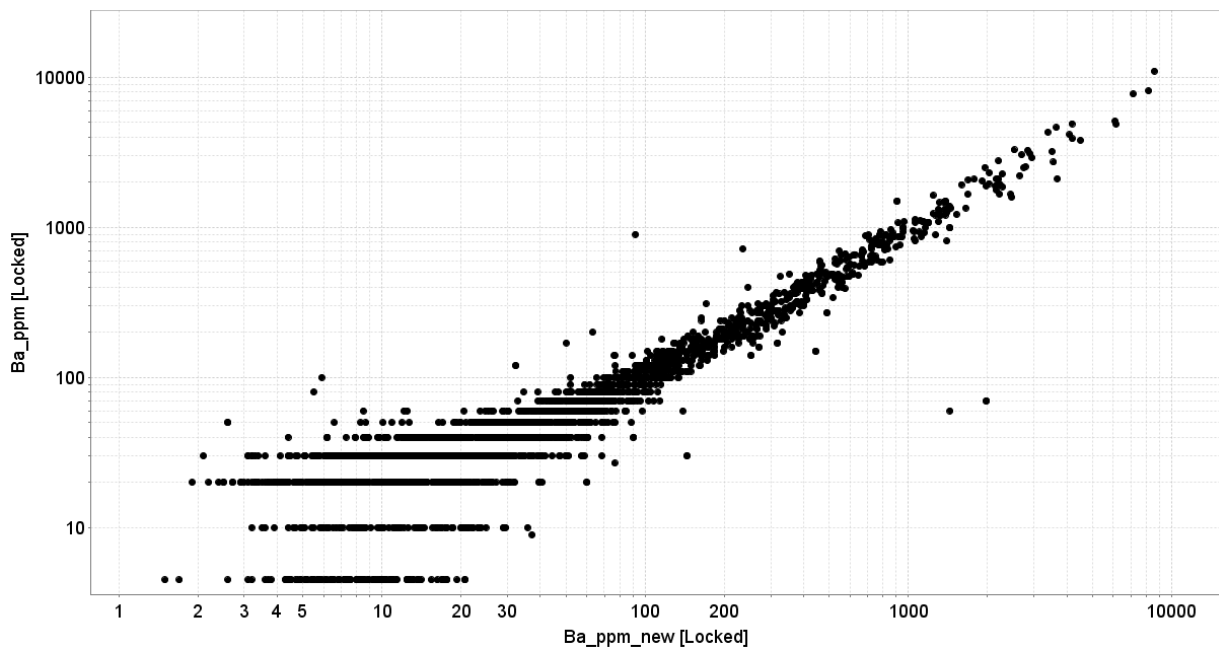


Figure 5 Diagram showing the values for the new versus original analysis for barium, demonstrating the improved precision through a lower detection limit.

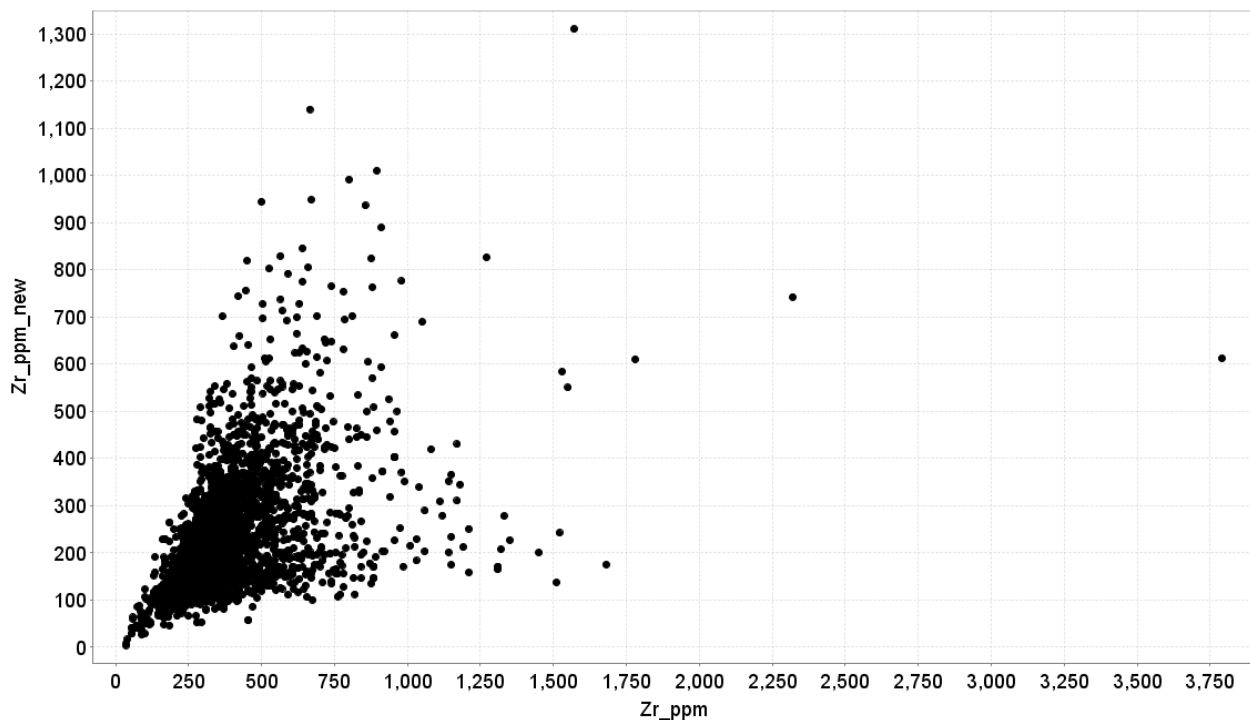


Figure 6 Diagram showing the values for the original versus new analysis for zirconium, showing large discrepancy due to different digest methods (fusion vs multi-acid digest).

3.1.2 New data characteristics and regional distribution patterns

Table 2 shows the univariate characteristics of the newly analysed laterite samples. The spatial distribution patterns for the elements of interest are shown in Figure 7 through to Figure 28. Trends and zones where elements are enriched or anomalous present new information for exploration targeting. These patterns are noted in Section 4.

Table 2 Univariate statistics for new data of samples that have results above detection limit. Units are ppm except for Pt in ppb, bdl = below detection limit.

Elements	n	n [bdl]	Min	Max	Mean	Median
Ag_new	2288	150	0.01	4.84	0.07	0.04
Ba_new	2438	0	0.01	8250	133.2	26.9
Be_new	2422	16	0.2	10.8	1.02	0.9
Co_new	2438	0	0.5	143	6.9	4.9
Cr_new	2438	0	0.01	8860	374	198
Cs_new	2361	77	0.1	27.9	0.6	0.4
Dy_new	2438	0	0.15	21.3	1.08	0.84
Hf_new	2438	0	0.08	31	6.2	5.6
Hg_new	503	1935	0.05	3.4	0.12	0.08
Ho_new	2438	0	0.03	3.9	0.20	0.15
Li_new	2436	2	0.7	121	19.0	17.2
Nb_new	2438	0	0.15	224	13.4	11.4
Pt_new	2218	220	1	86	9.2	7
Rb_new	2435	3	0.1	262	9.1	4.9
Re_new	991	1447	0.5	38	1.1	0.9
Sc_new	2420	18	2	330	19.9	16
Sn_new	2438	0	0.3	35.9	2.5	2.1
Ta_new	2420	18	0.01	30.8	1.12	0.89
Th_new	2438	0	1.31	761	106	84.7
U_new	2438	0	0.12	57.3	6.32	5.05
W_new	2437	1	0.1	135	1.63	1
Zr_new	2438	0	4	1340	236	201

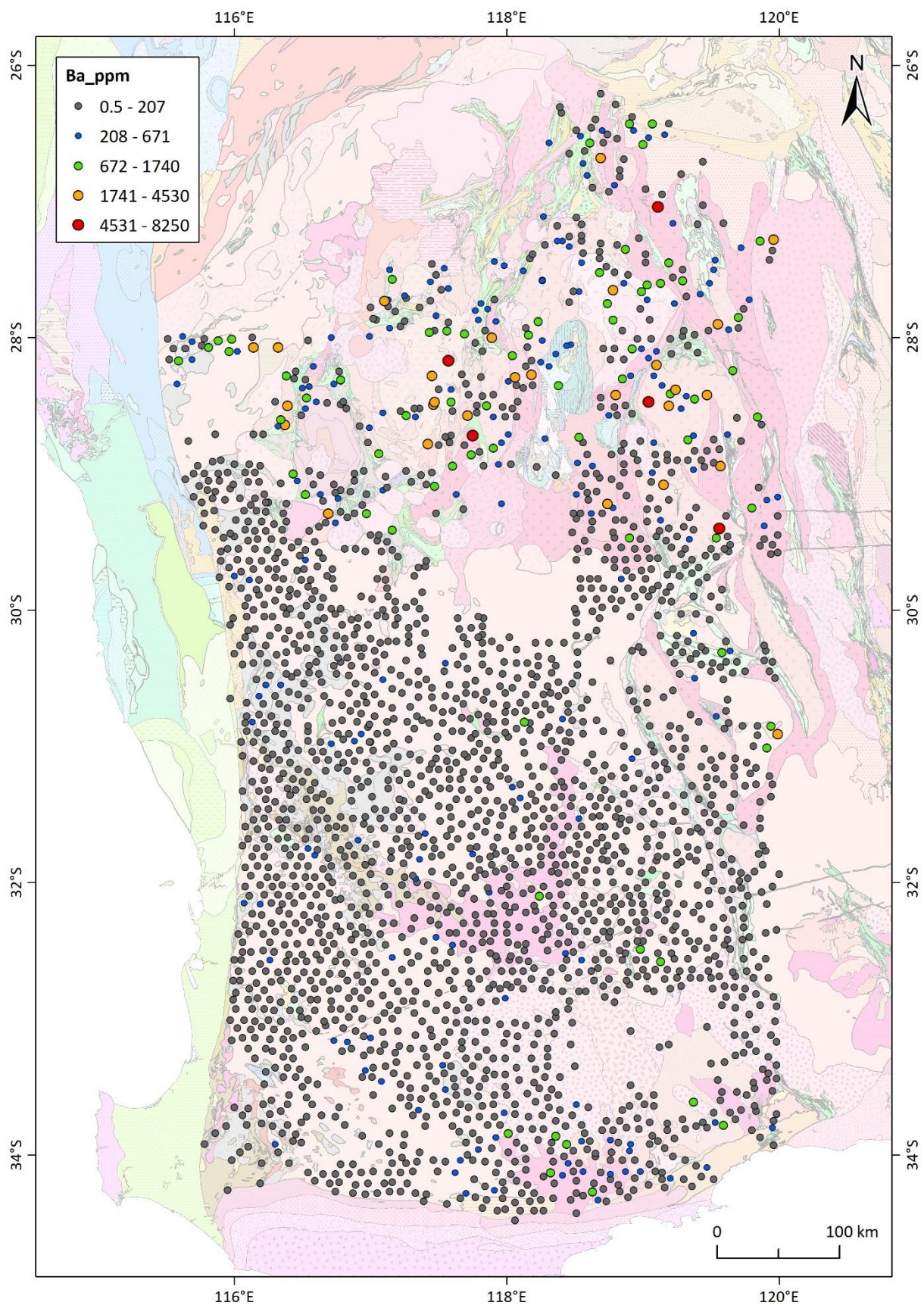


Figure 7 Barium distribution in the SW Yilgarn with 500K interpreted geology.

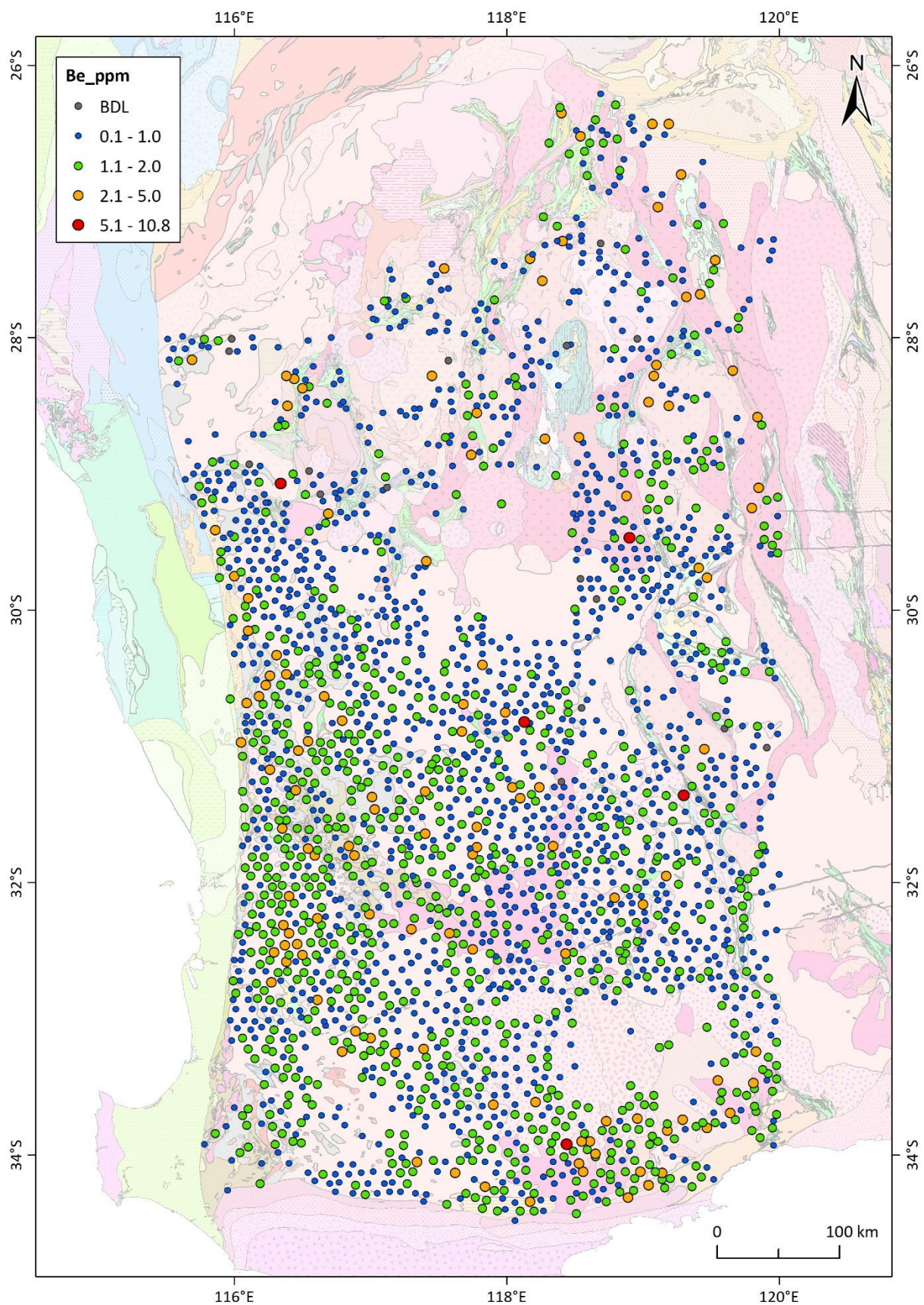


Figure 8 Beryllium distribution in the SW Yilgarn with 500K interpreted geology.

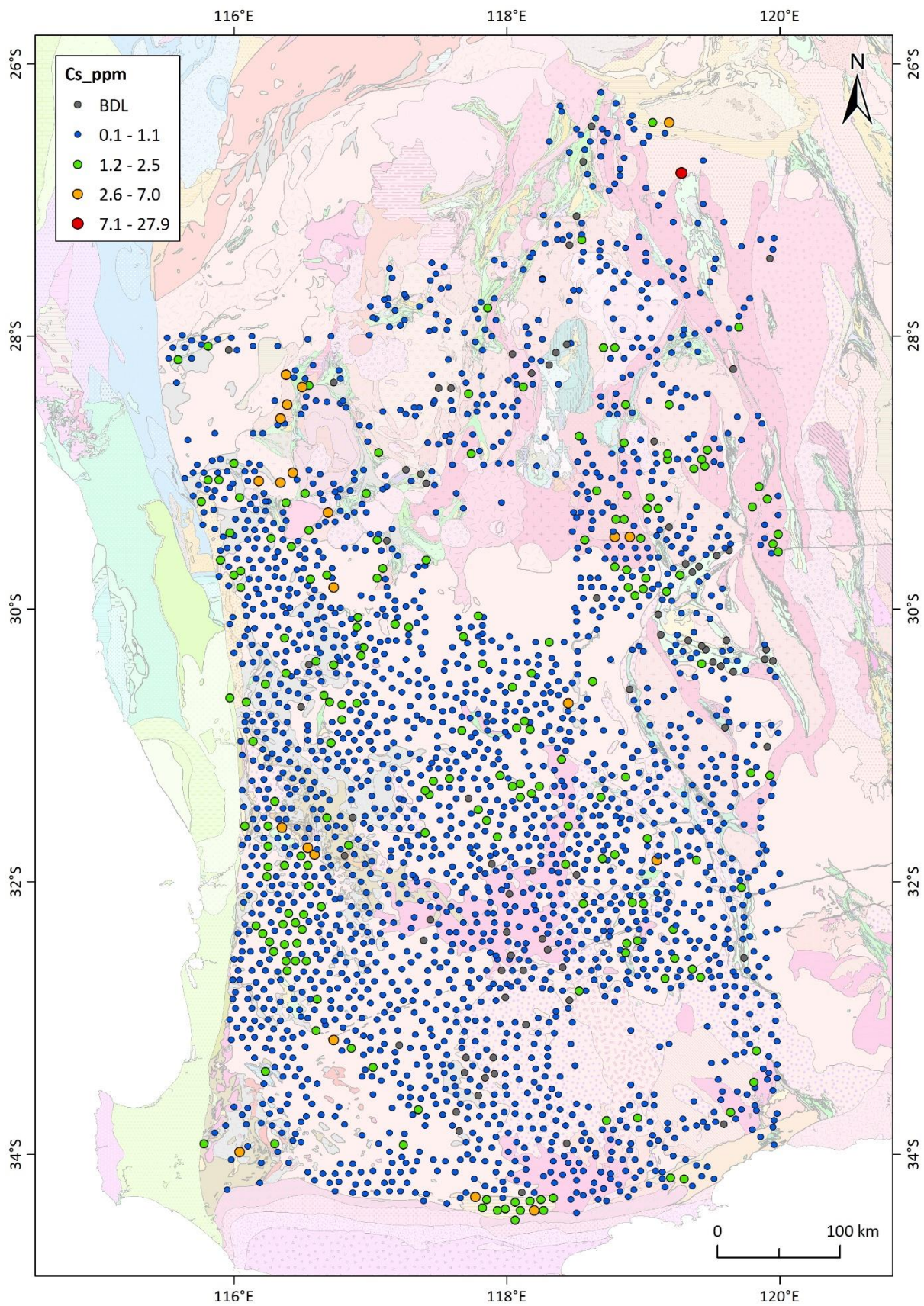


Figure 9 Caesium distribution in the SW Yilgarn with 500K interpreted geology.

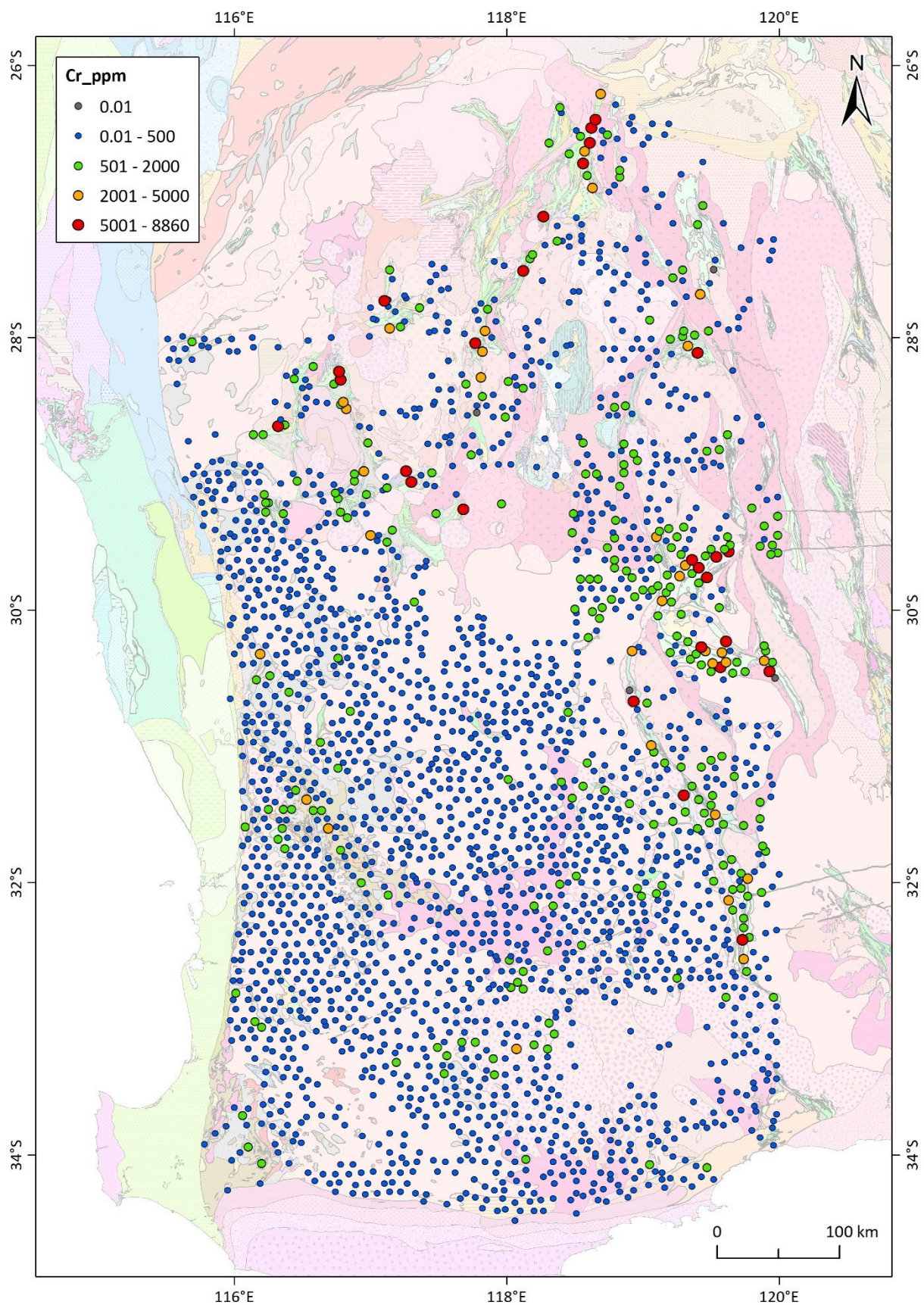


Figure 10 Chromium distribution in the SW Yilgarn with 500K interpreted geology.

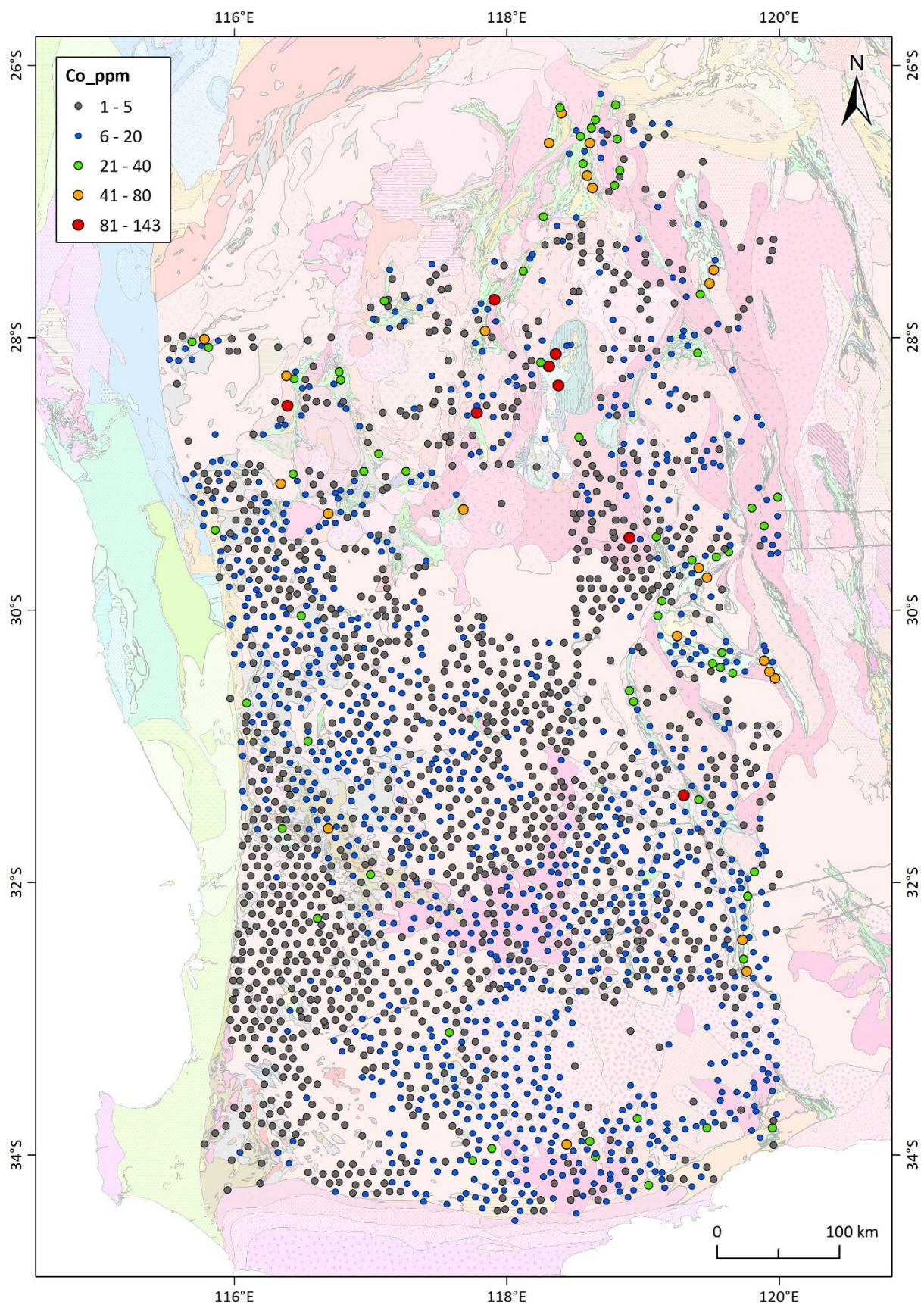


Figure 11 Cobalt distribution in the SW Yilgarn with 500K interpreted geology.

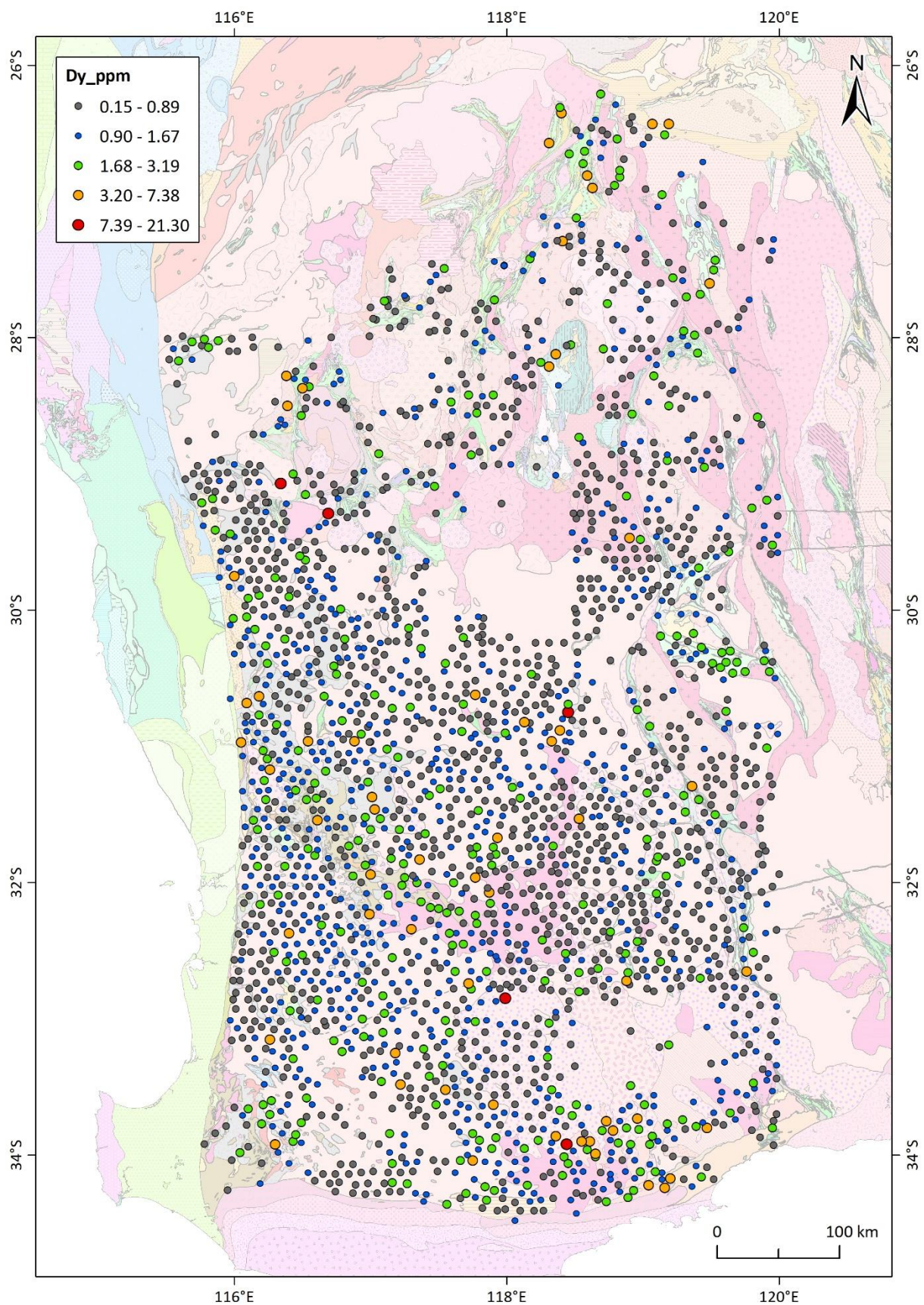


Figure 12 Dysprosium distribution in the SW Yilgarn with 500K interpreted geology.

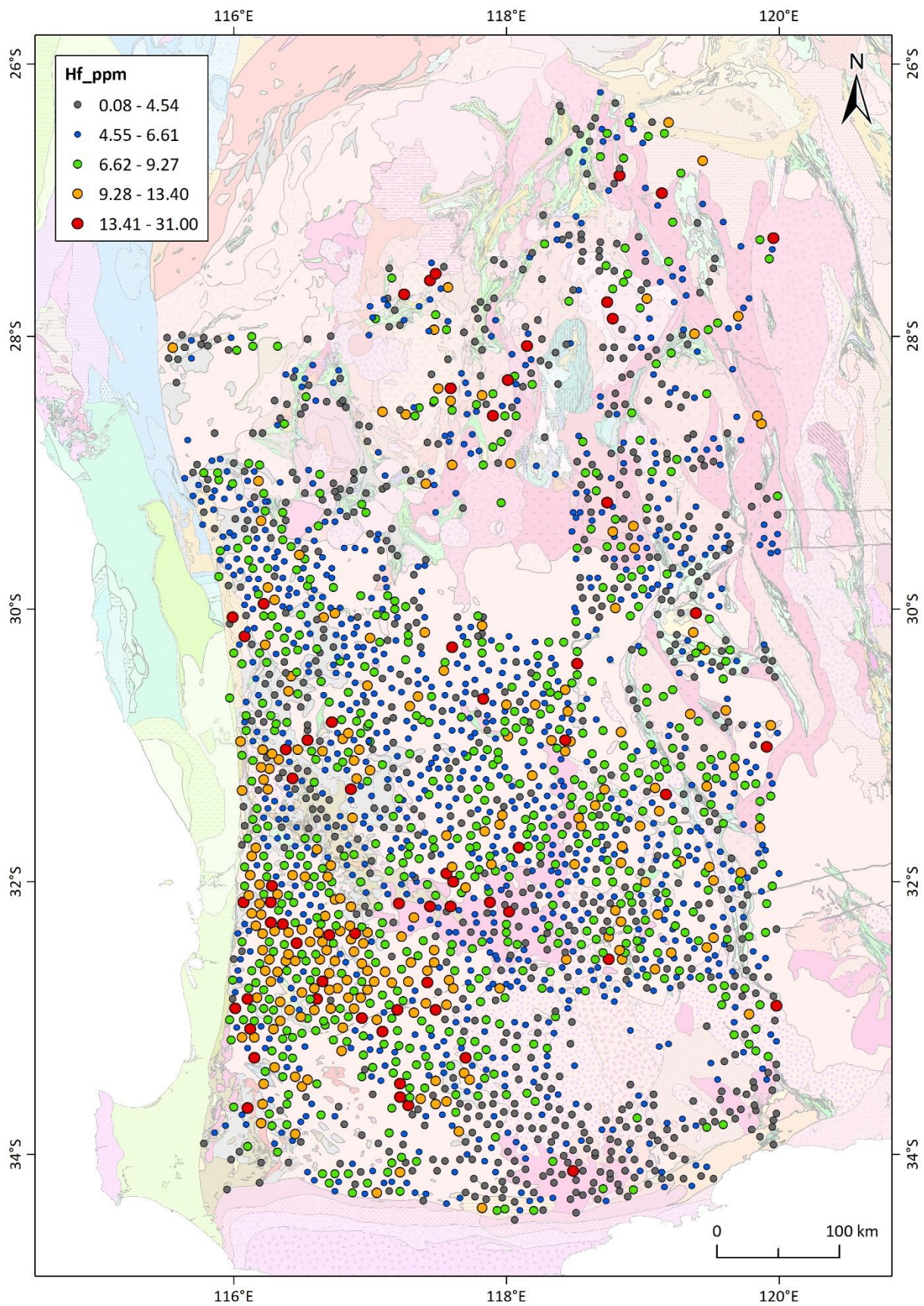


Figure 13 Hafnium distribution in the SW Yilgarn with 500K interpreted geology.

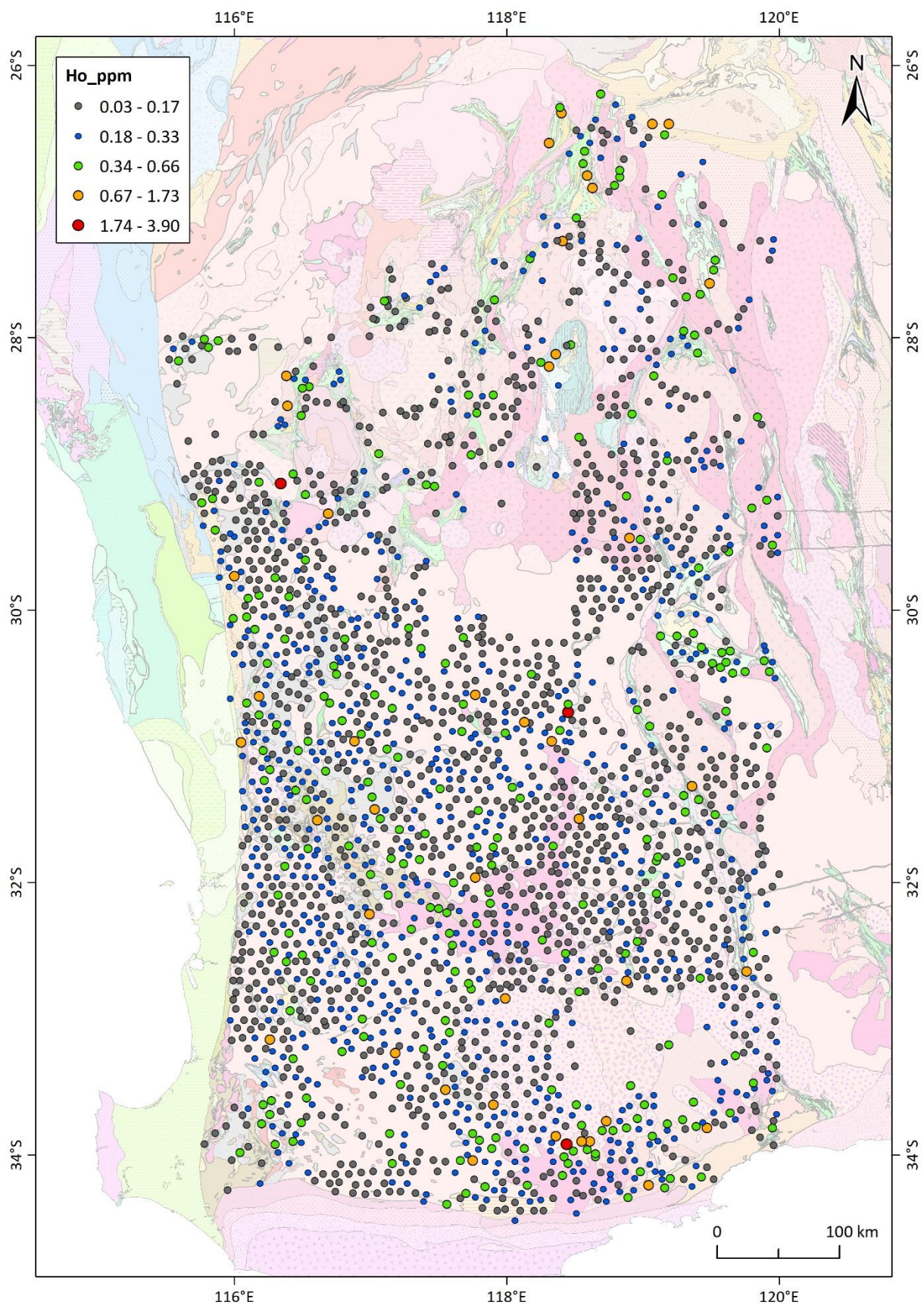


Figure 14 Holmium distribution in the SW Yilgarn with 500K interpreted geology.

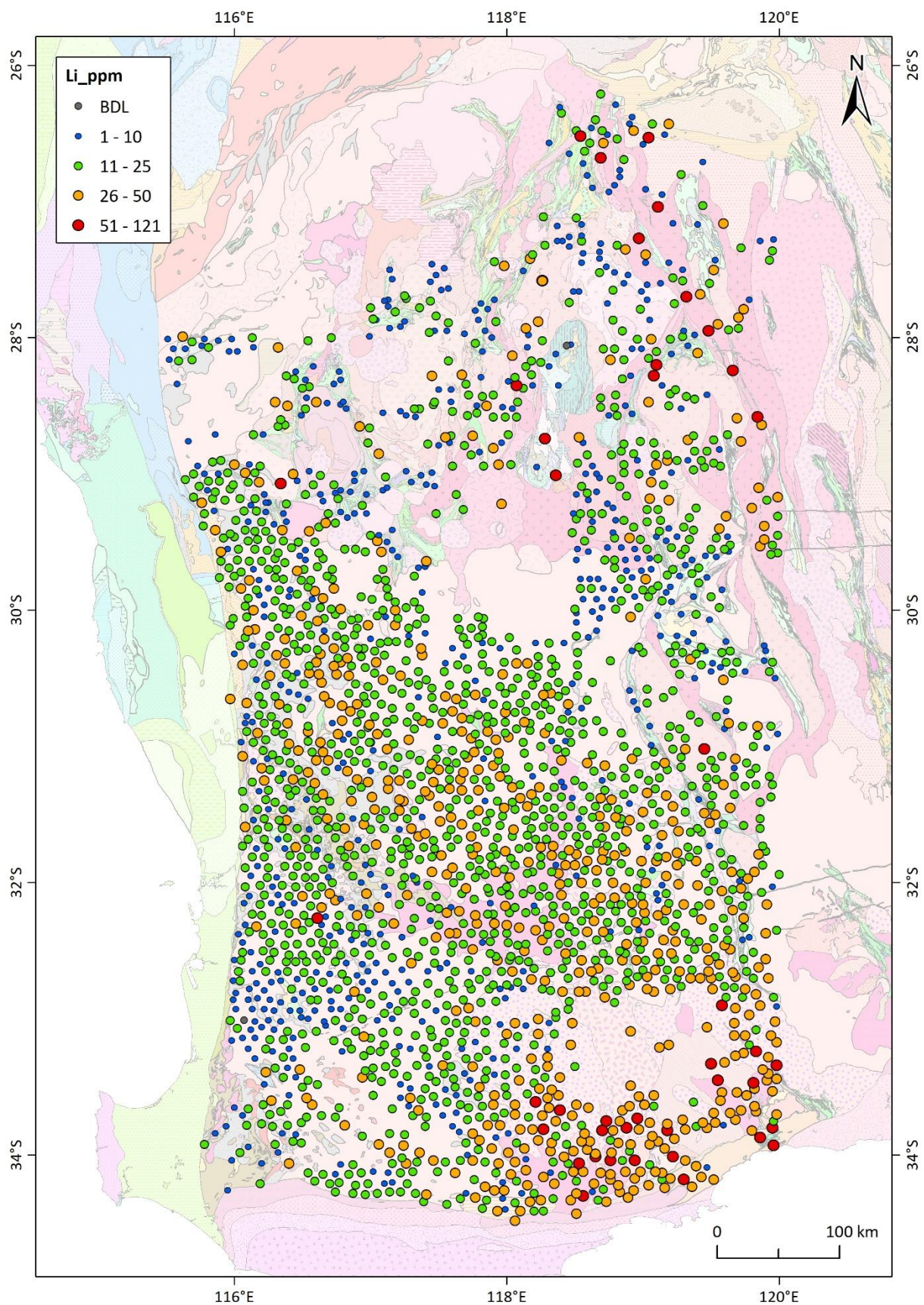


Figure 15 Lithium distribution in the SW Yilgarn with 500K interpreted geology.

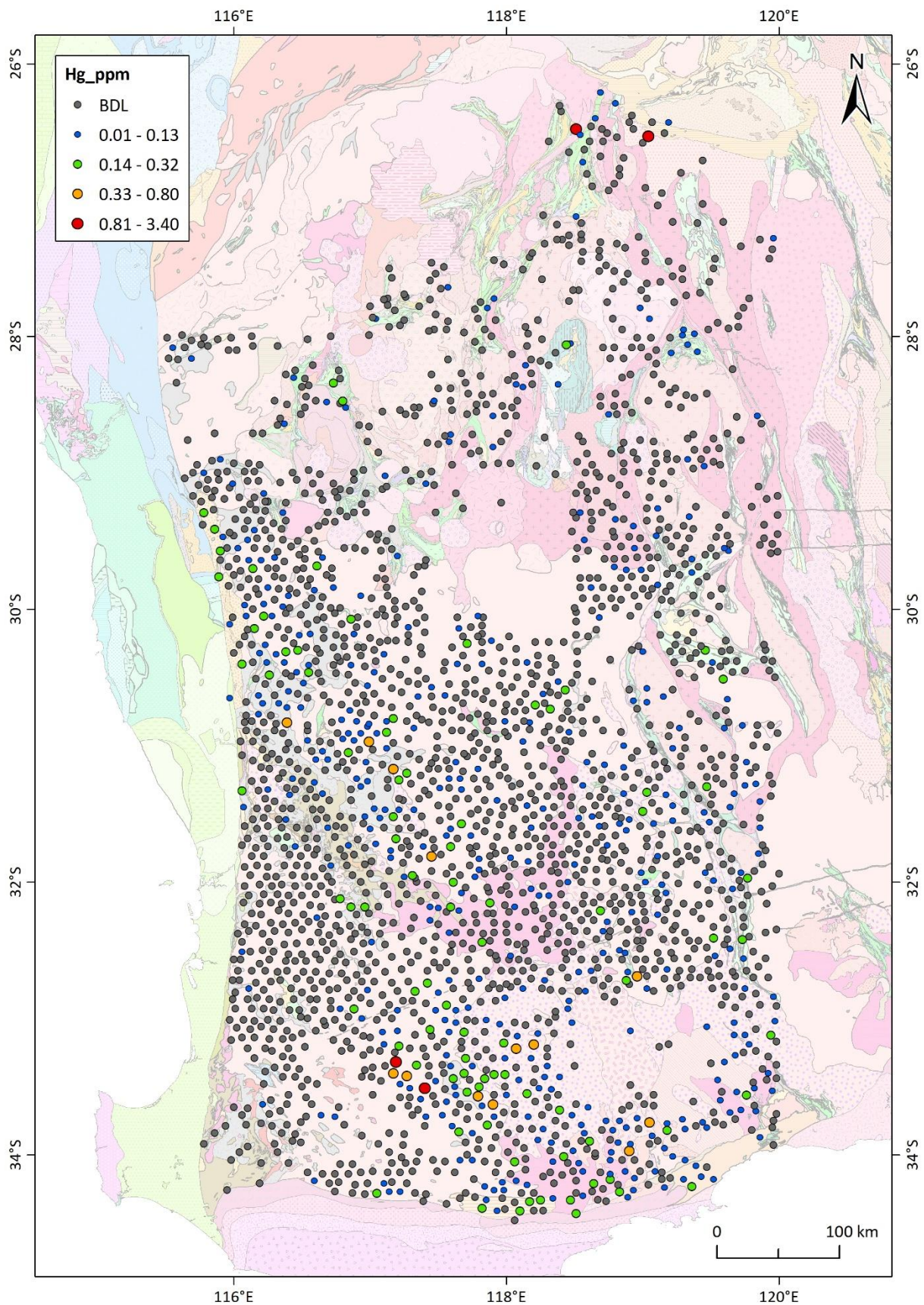


Figure 16 Mercury distribution in the SW Yilgarn with 500K interpreted geology.

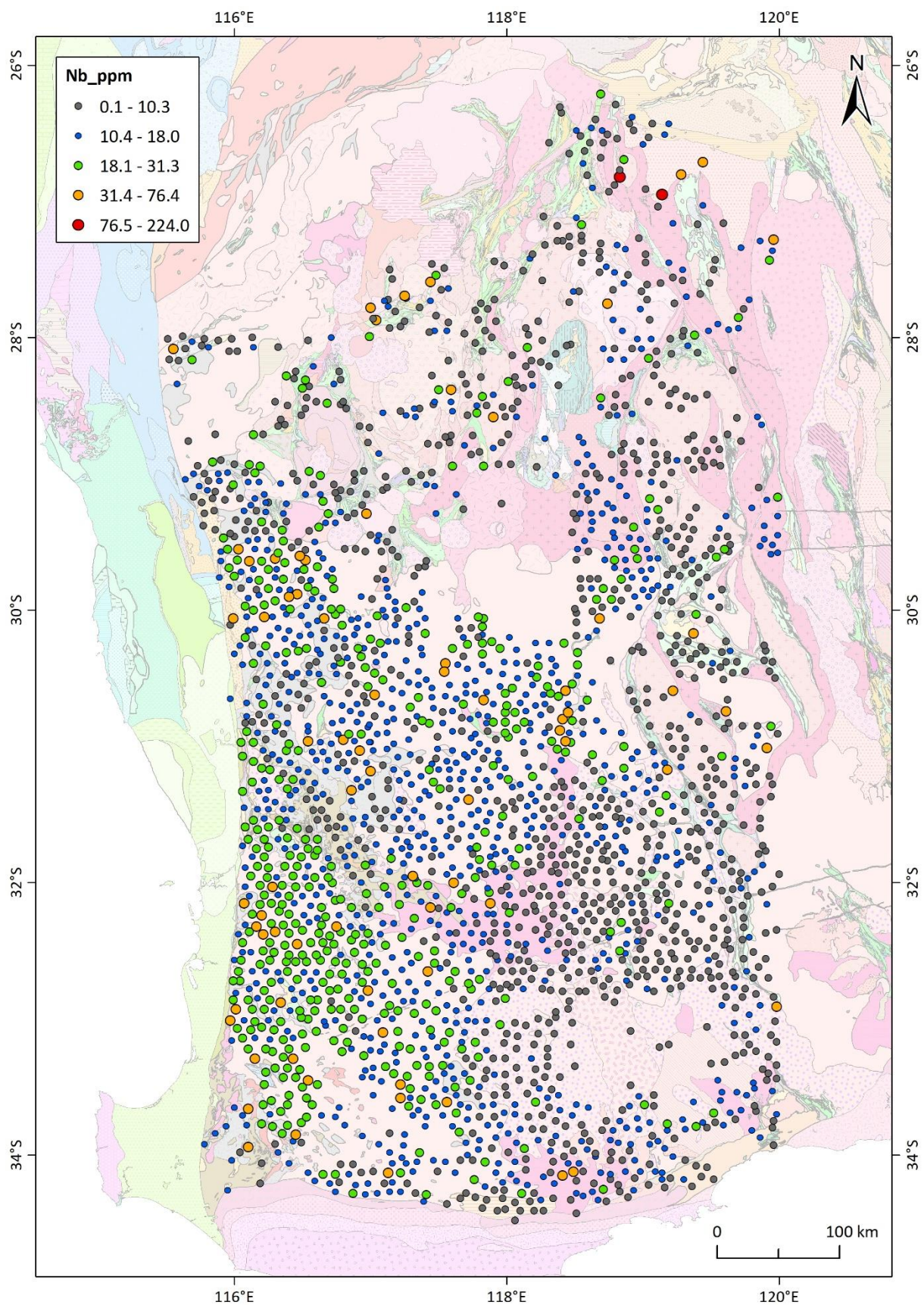


Figure 17 Niobium distribution in the SW Yilgarn with 500K interpreted geology.

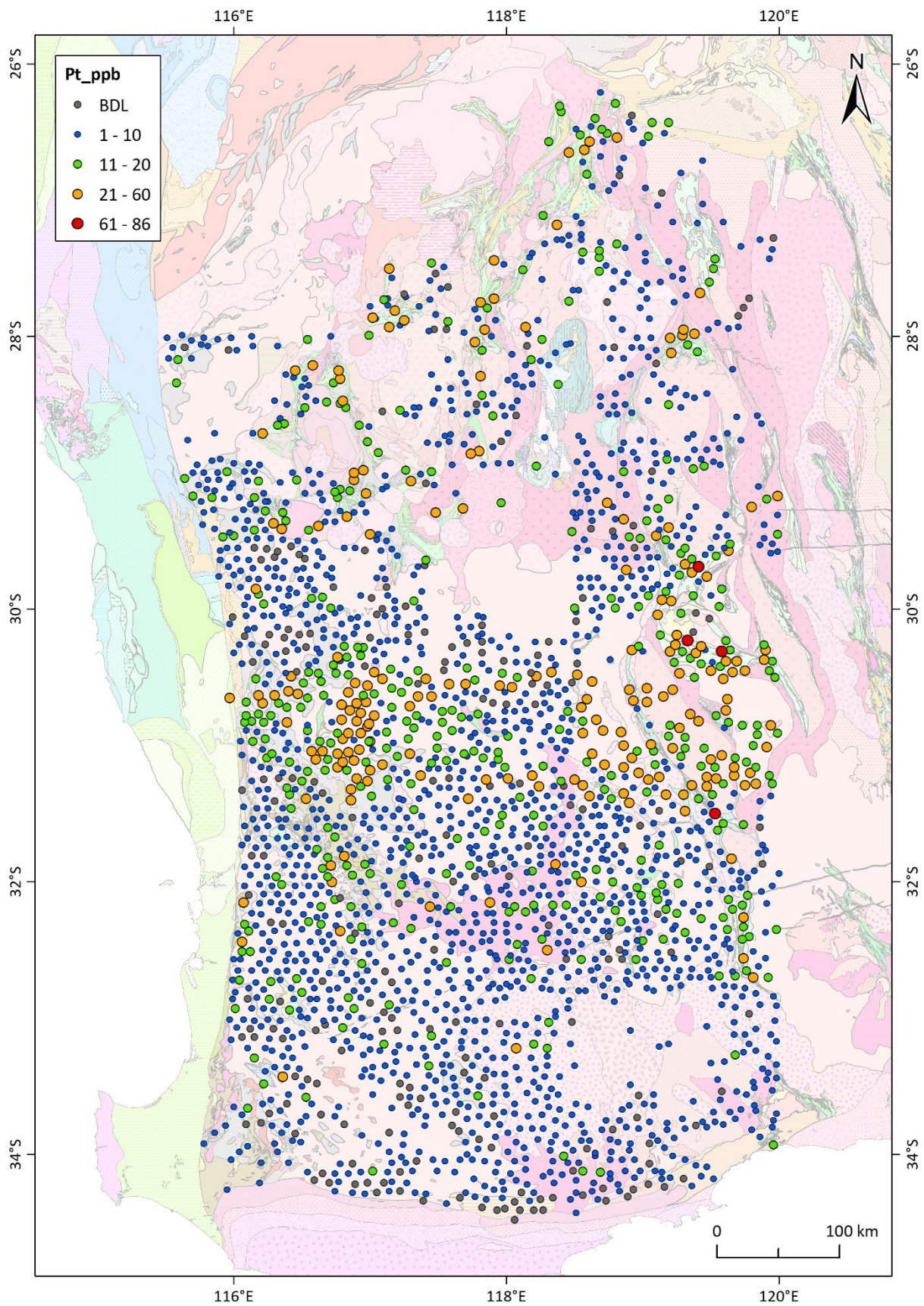


Figure 18 Platinum distribution in the SW Yilgarn with 500K interpreted geology.

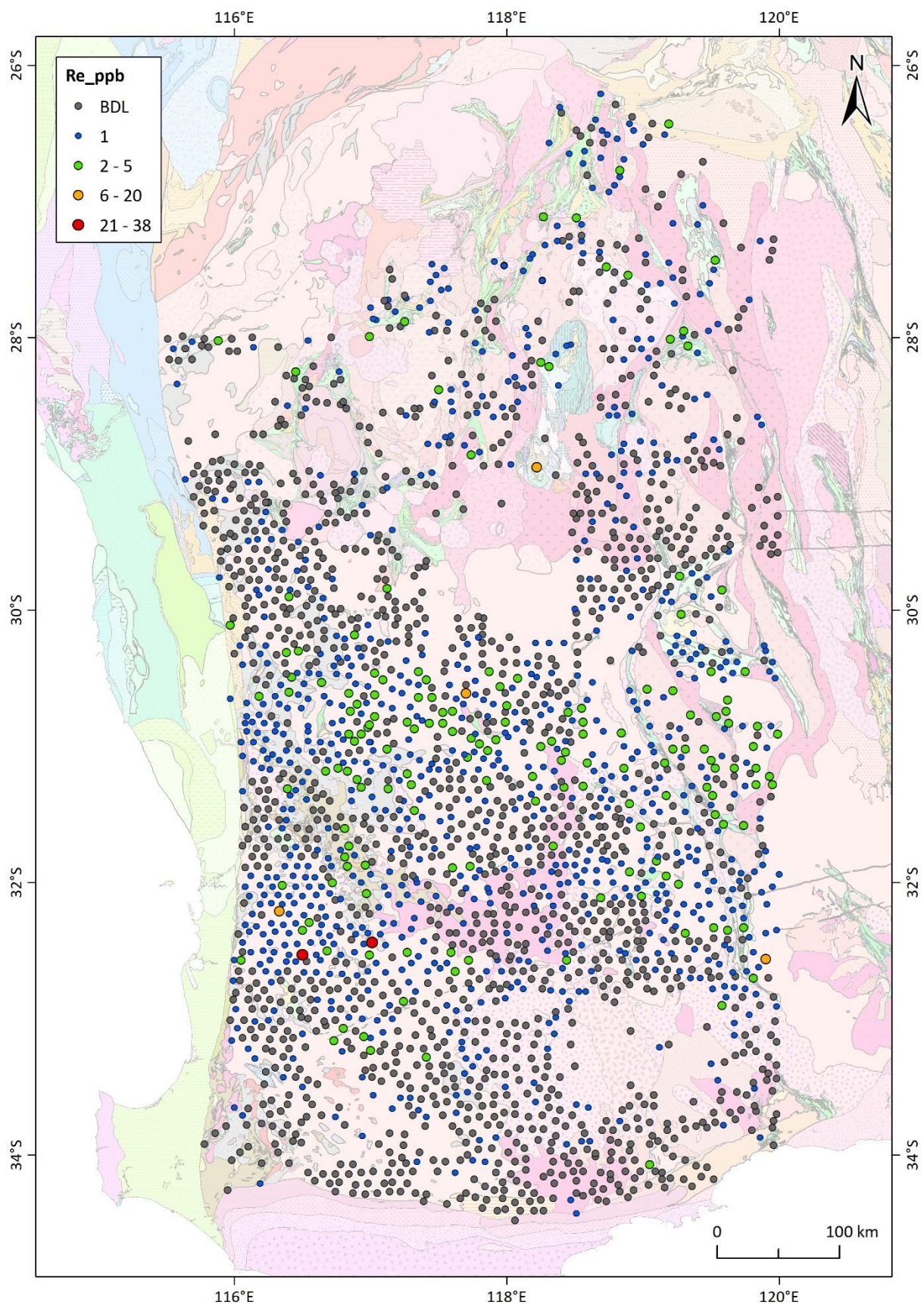


Figure 19 Rhenium distribution in the SW Yilgarn with 500K interpreted geology.

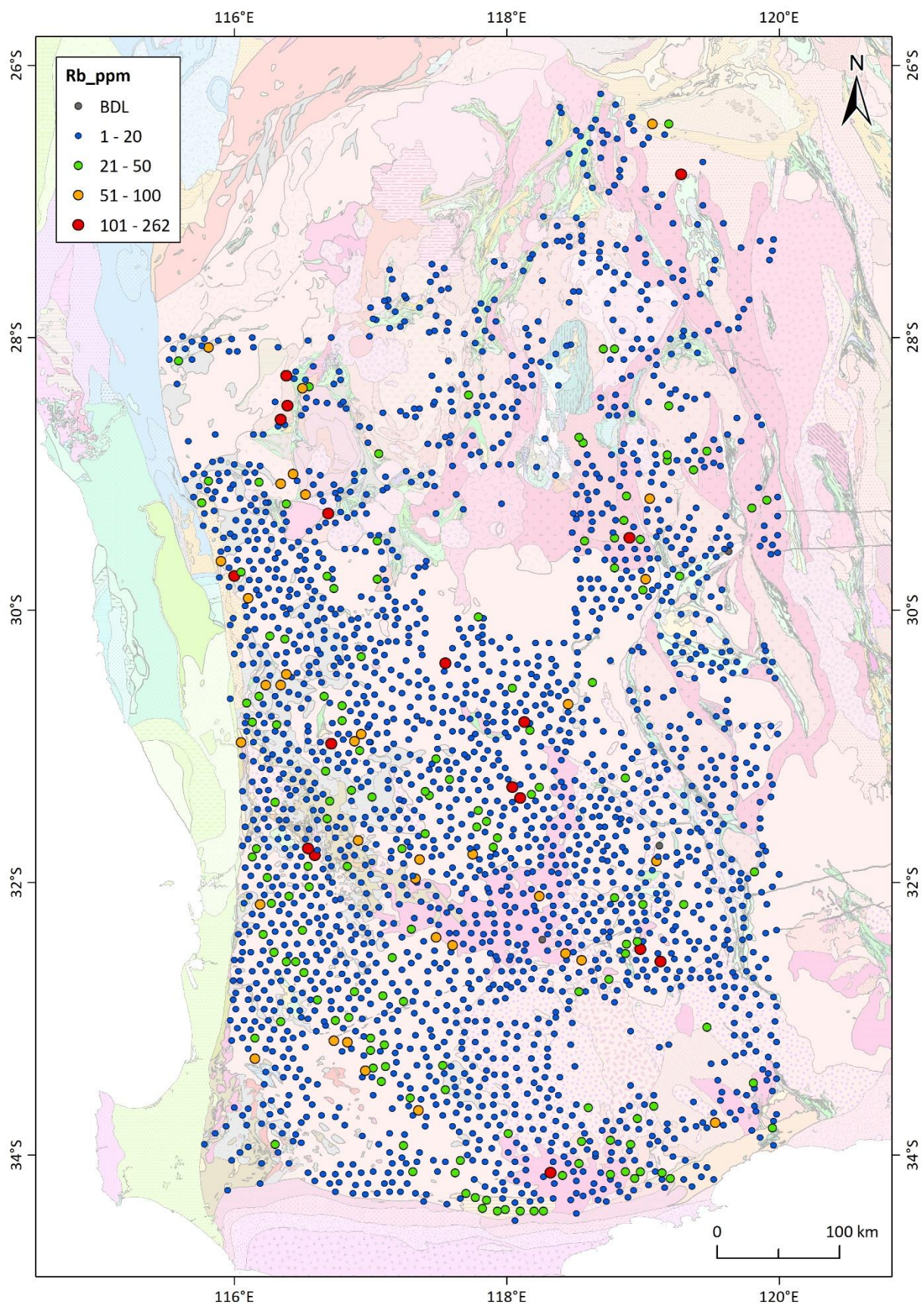


Figure 20 Rubidium distribution in the SW Yilgarn with 500K interpreted geology.

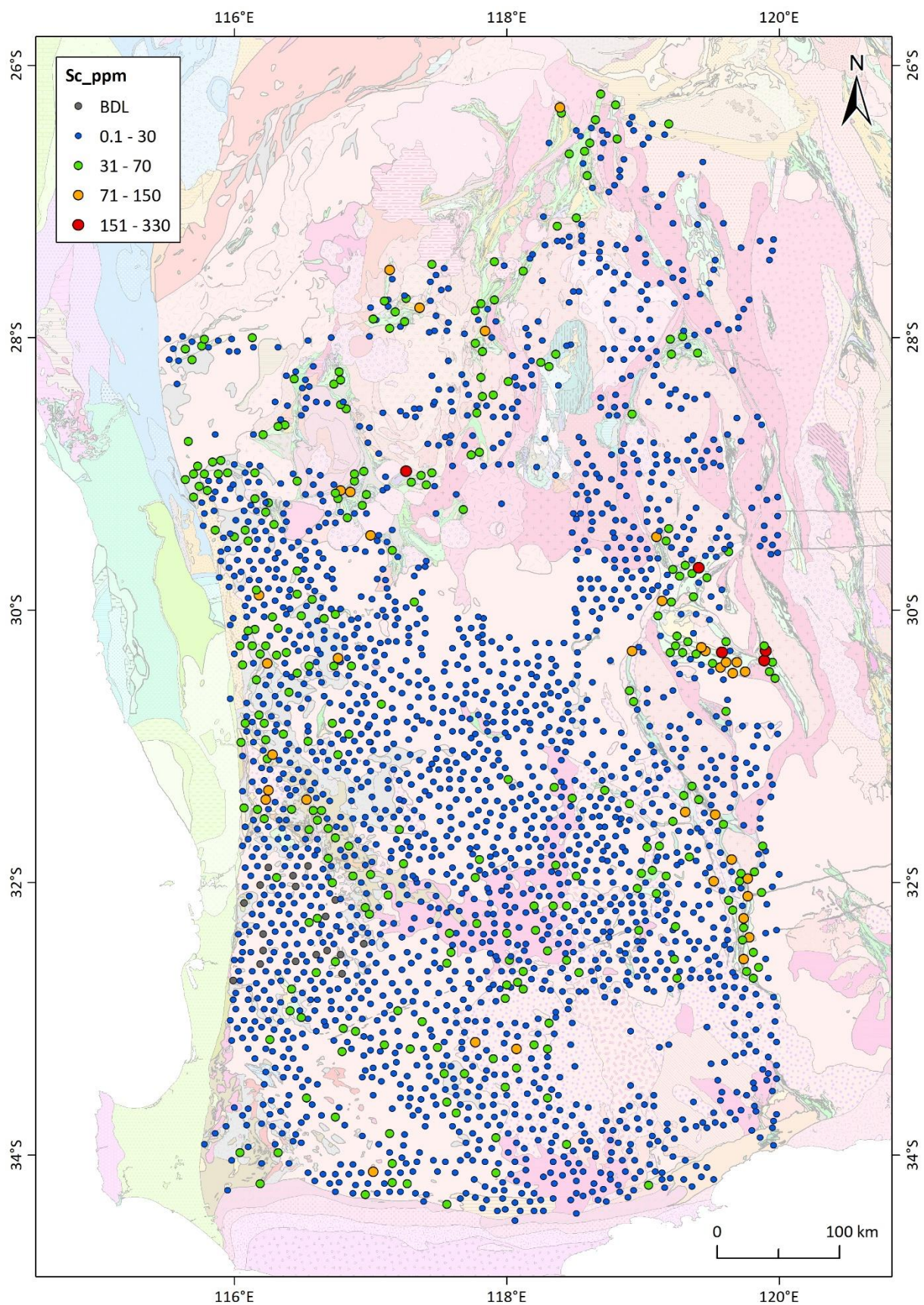


Figure 21 Scandium distribution in the SW Yilgarn with 500K interpreted geology.

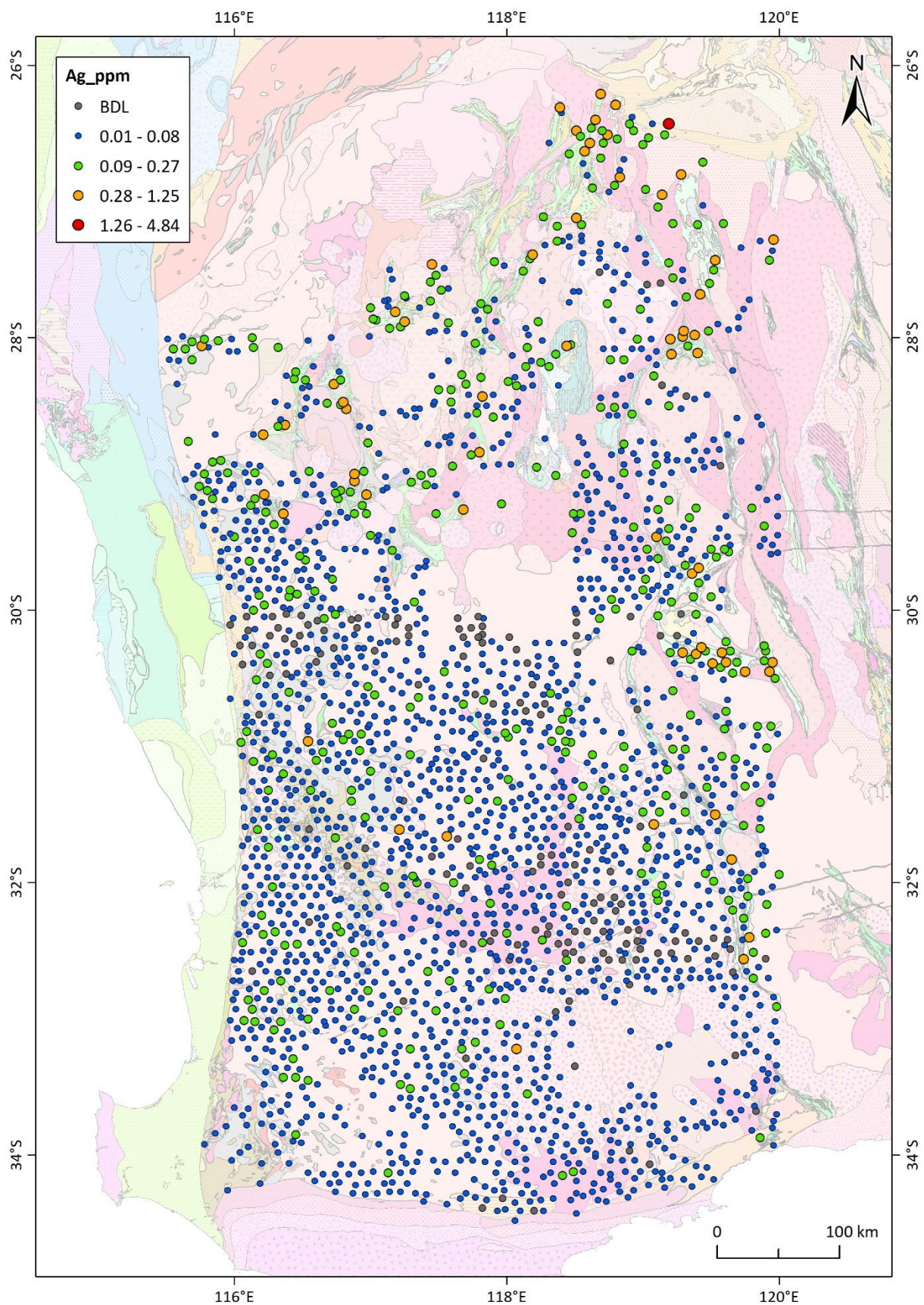


Figure 22 Silver distribution in the SW Yilgarn with 500K interpreted geology.

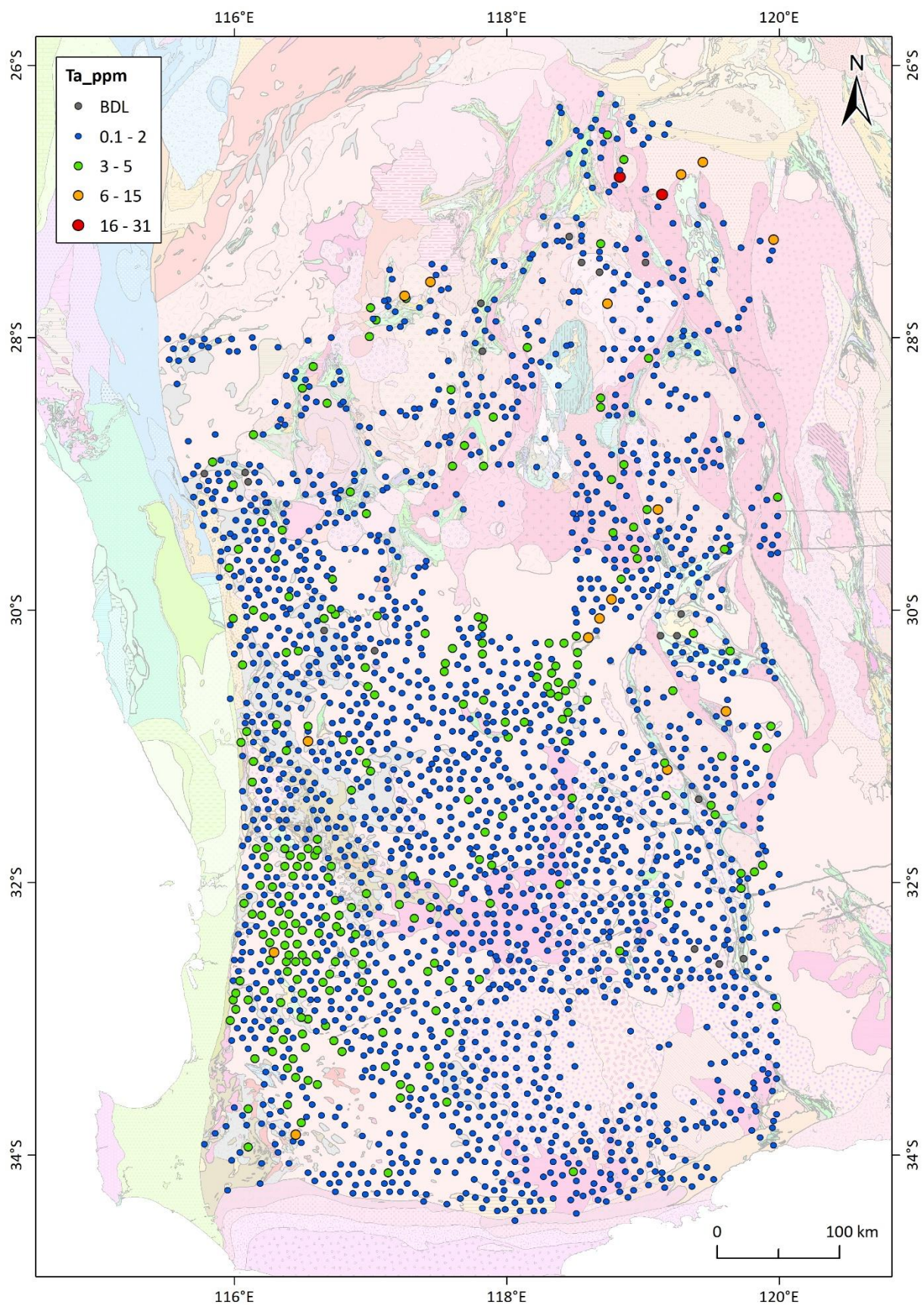


Figure 23 Tantalum distribution in the SW Yilgarn with 500K interpreted geology.

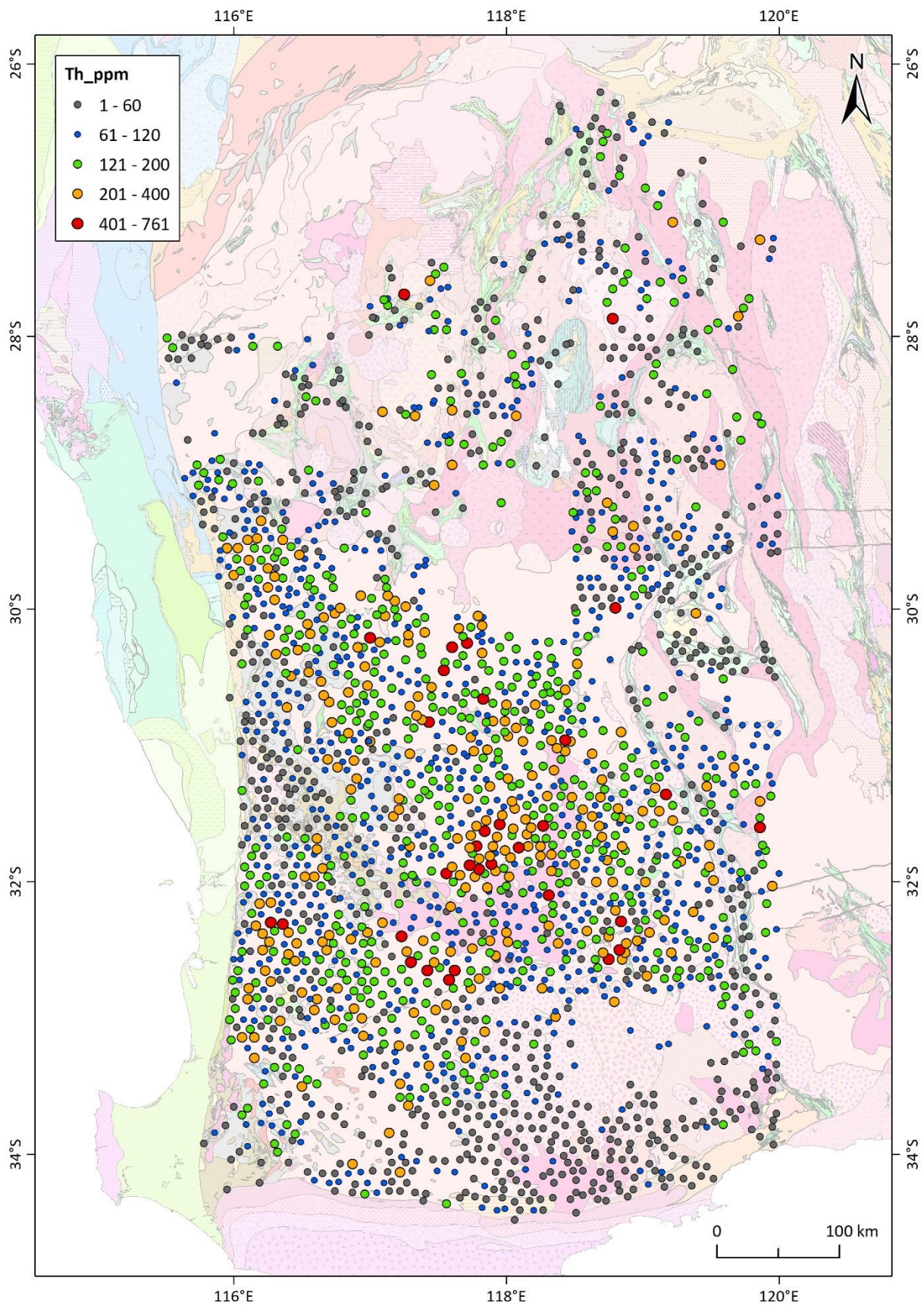


Figure 24 Thorium distribution in the SW Yilgarn with 500K interpreted geology.

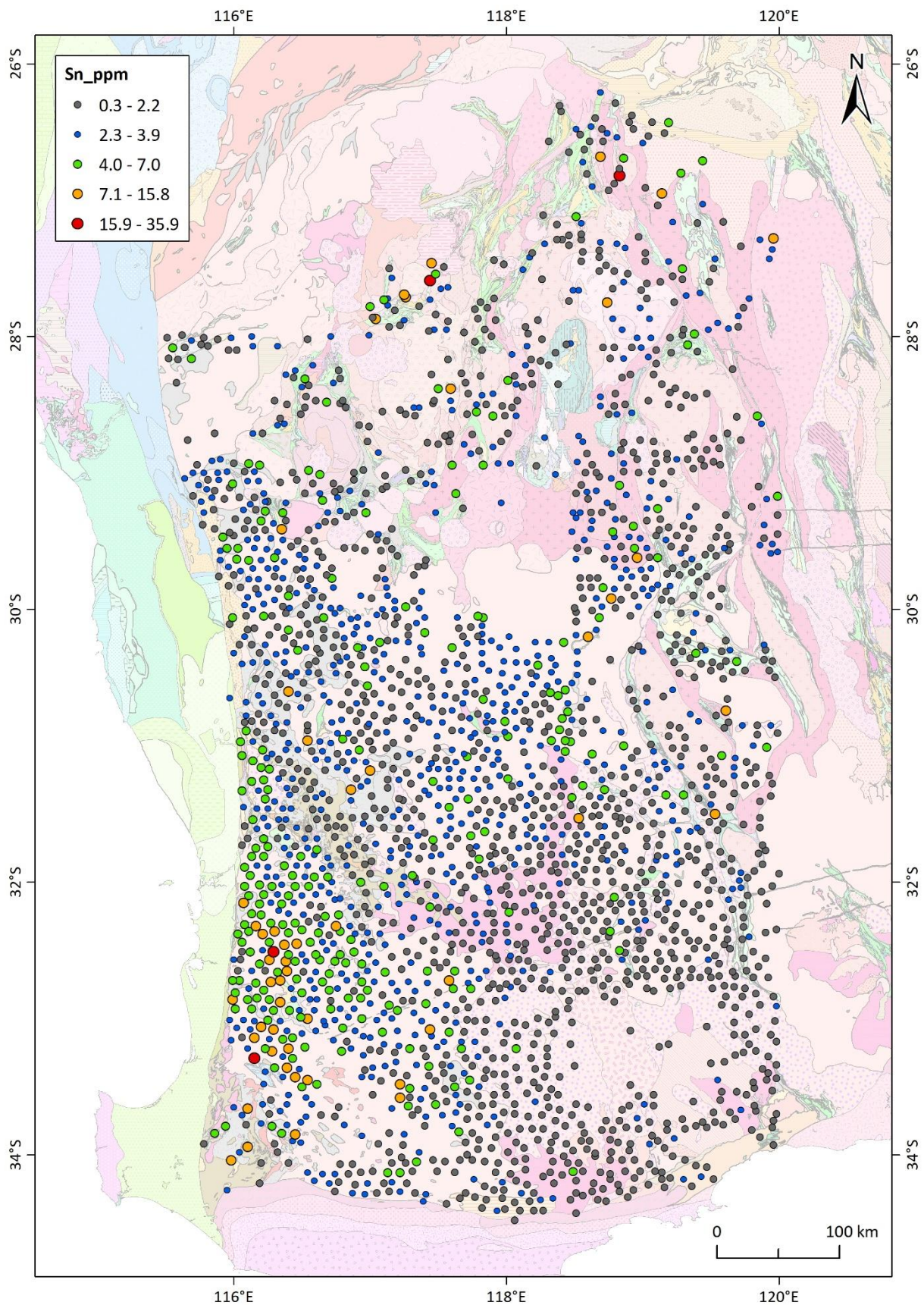


Figure 25 Tin distribution in the SW Yilgarn with 500K interpreted geology.

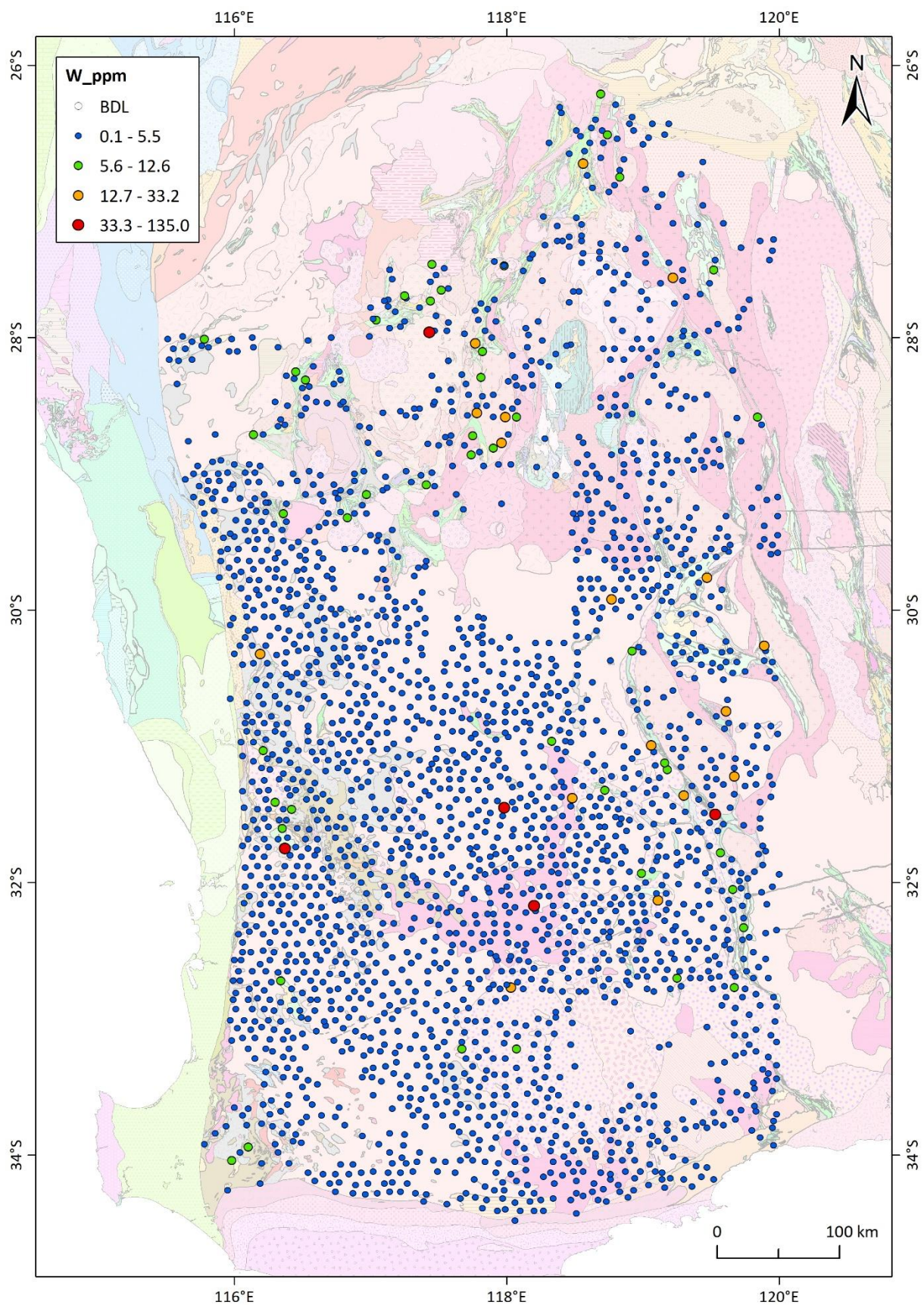


Figure 26 Tungsten distribution in the SW Yilgarn with 500K interpreted geology.

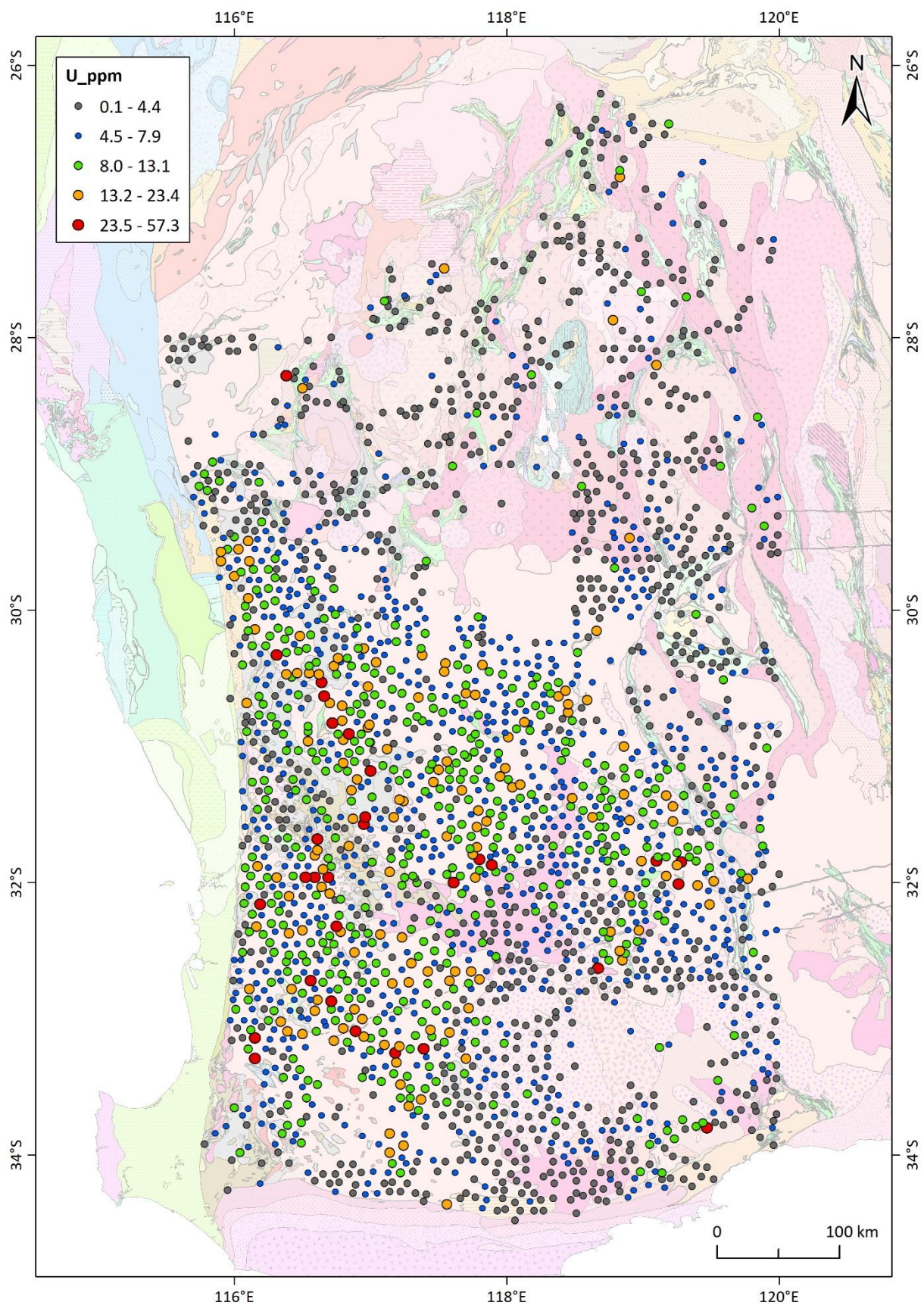


Figure 27 Uranium distribution in the SW Yilgarn with 500K interpreted geology.

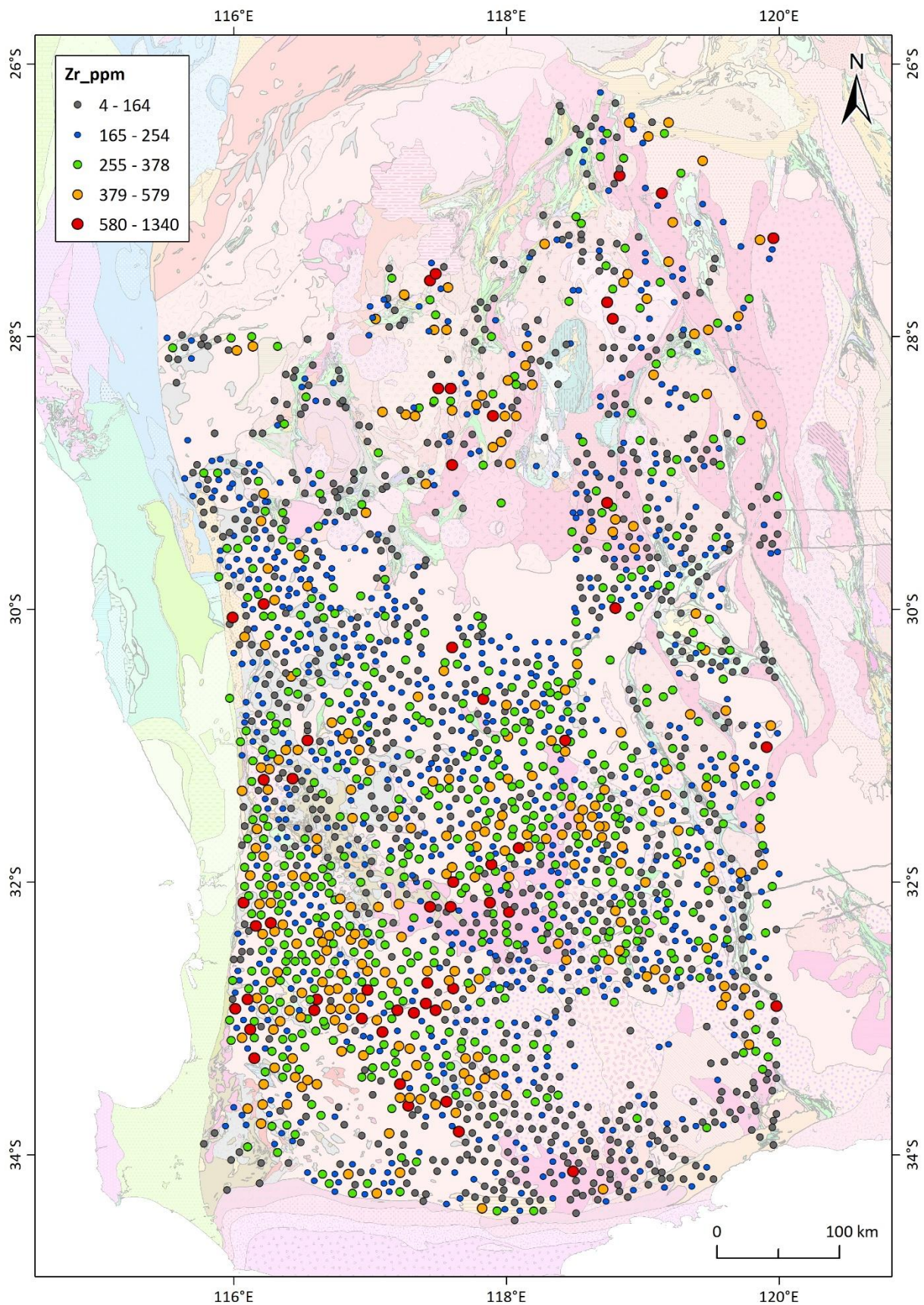


Figure 28 Zirconium distribution in the SW Yilgarn with 500K interpreted geology.

3.2 Mineralogy

3.2.1 Infrared Reflectance Spectroscopy

Fine grain size causes considerable scattering effects within the TIR wavelength range, which overwhelm most spectral features related to the minerals in this data set. However, the VNIR-SWIR wavelength range is less affected by the grain size, and relative mineral abundances for kaolinite, gibbsite, and iron oxides (goethite and hematite) could be delineated from the spectra. The spectra indicate mineralogy within laterite changes from the kaolinite and hematite abundant northeast towards the gibbsite and goethite abundant southwest (Figure 29 - Figure 31).

Scope = Mask(Final Mask); 2638 Points, $r=-0.00183$; Aux: Kaolinite weights (uTSAS)

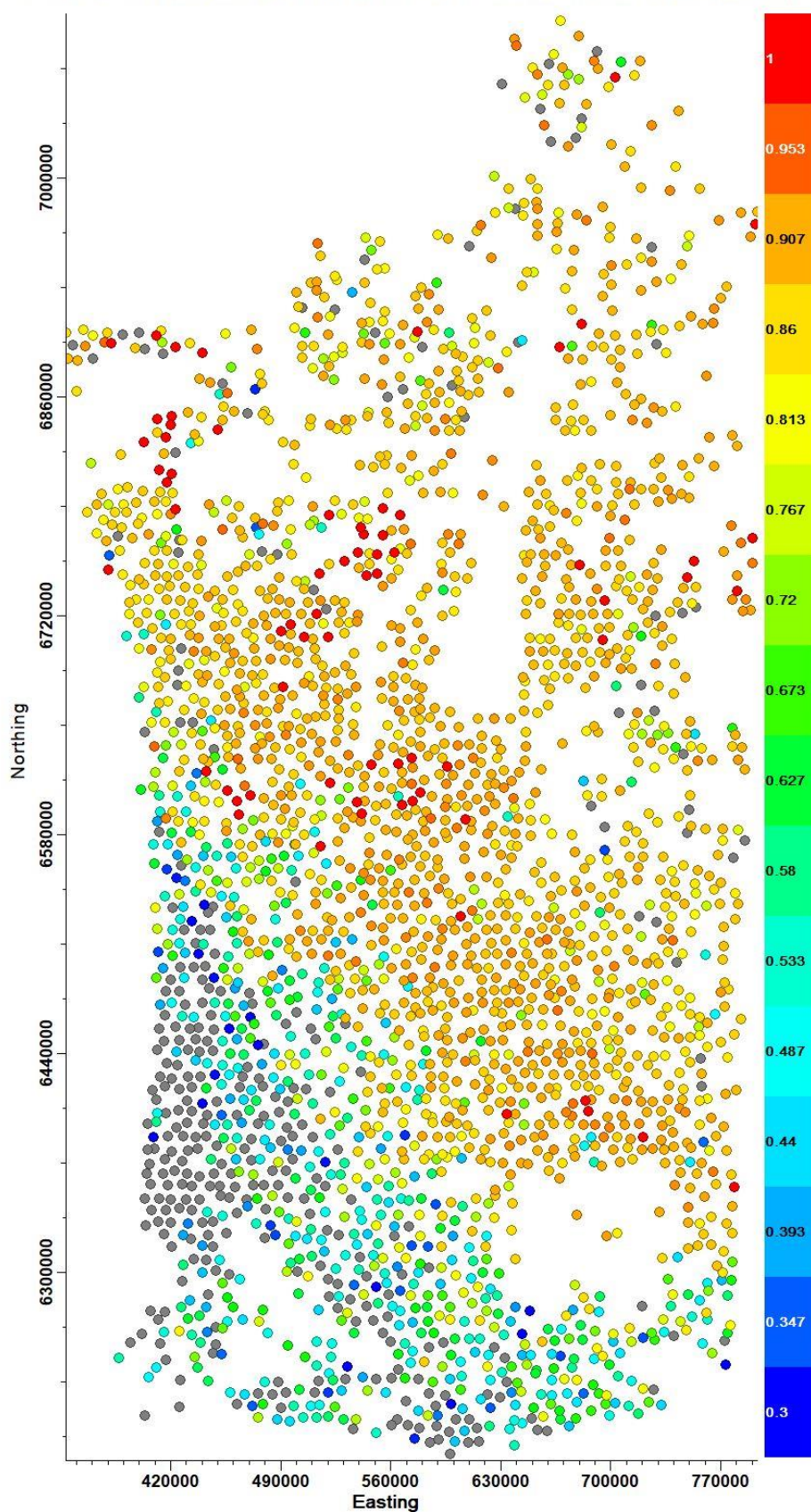


Figure 29. Kaolinite relative abundance (qualitative weight in TSA output of identified phases only) delineated from HyLogger-3™ data indicating significant spatial difference in the mineralogic composition of the laterite samples between southwest and northeast of the sampled area of the Yilgarn Craton.

Scope = Mask(Final Mask); 2638 Points, $r=-0.00183$; Aux: Gibbsite weights (uTSAS)

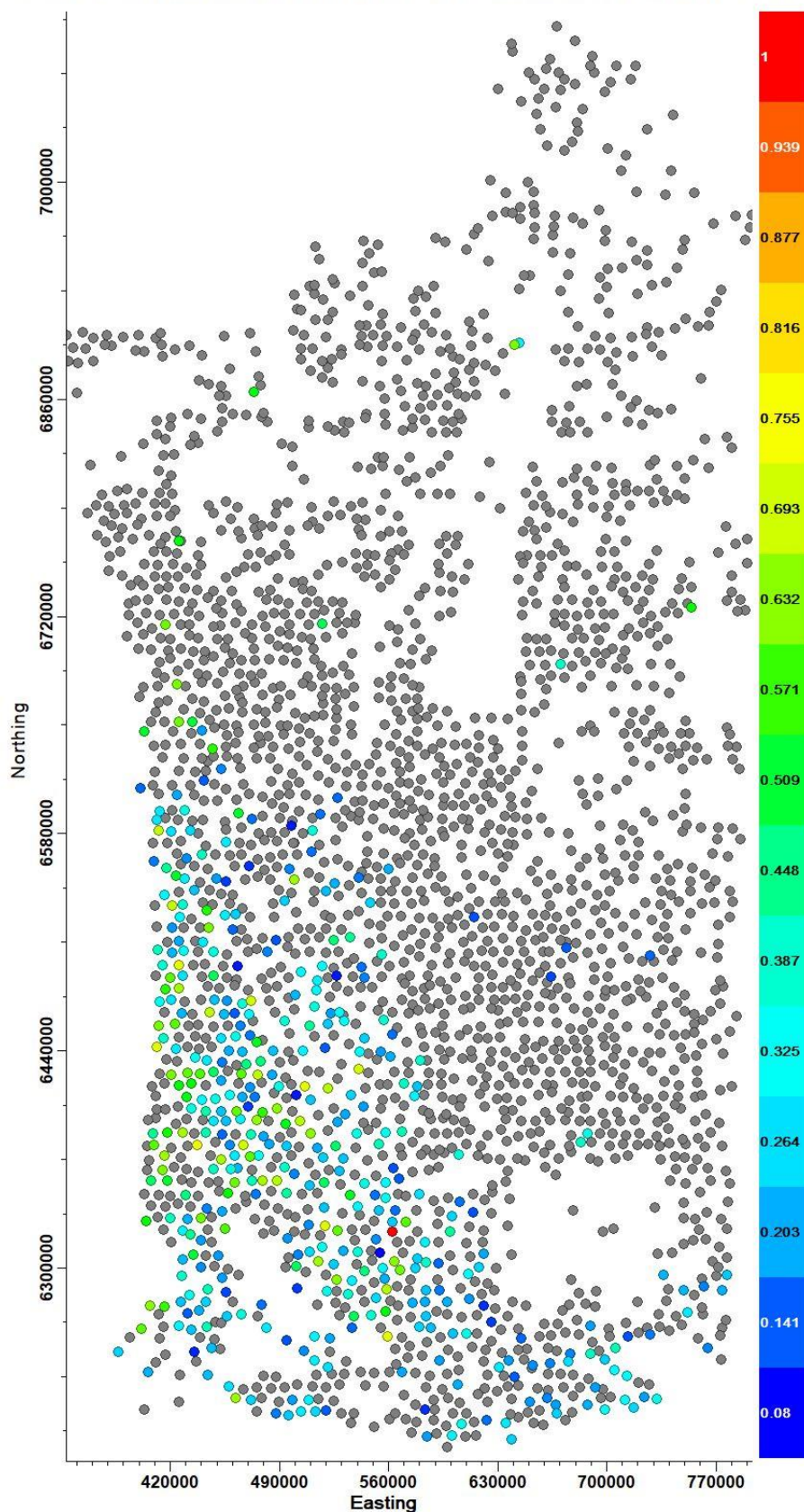


Figure 30. Gibbsite relative abundance (qualitative weight in TSA output of identified phases only) delineated from HyLogger-3™ data indicating significant spatial difference in the mineralogic composition of the laterite samples between southwest and northeast of the sampled area of the Yilgarn Craton

Scope = Mask(Final Mask); 2638 Points, $r=-0.00183$; Aux: Goethite weights (uTSAV)

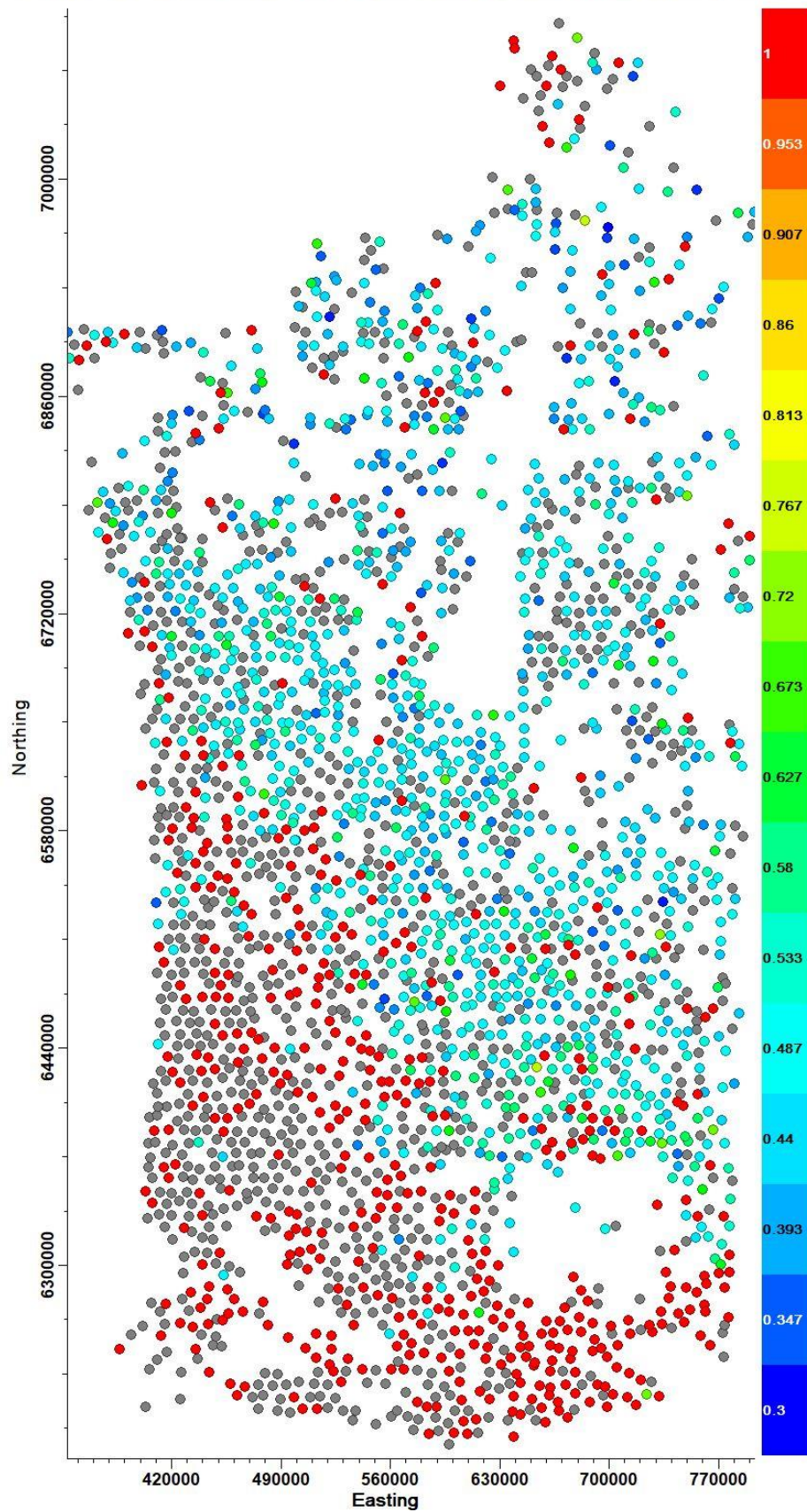


Figure 31. Goethite relative abundance (qualitative weight in TSA output of identified phases only) delineated from HyLogger-3 data indicating significant spatial difference in the mineralogic composition of the laterite samples between southwest and northeast of the sampled area of the Yilgarn Craton.

3.2.2 X-ray diffraction analysis

The results from the XRD analysis of 47 samples indicate that the mineralogy is dominated by quartz, the aluminium phases are kaolinite, gibbsite, boehmite and the iron phases are hematite, goethite (Figure 32 - **Error! Reference source not found.**).

104666 (Coupled TwoTheta/Theta)

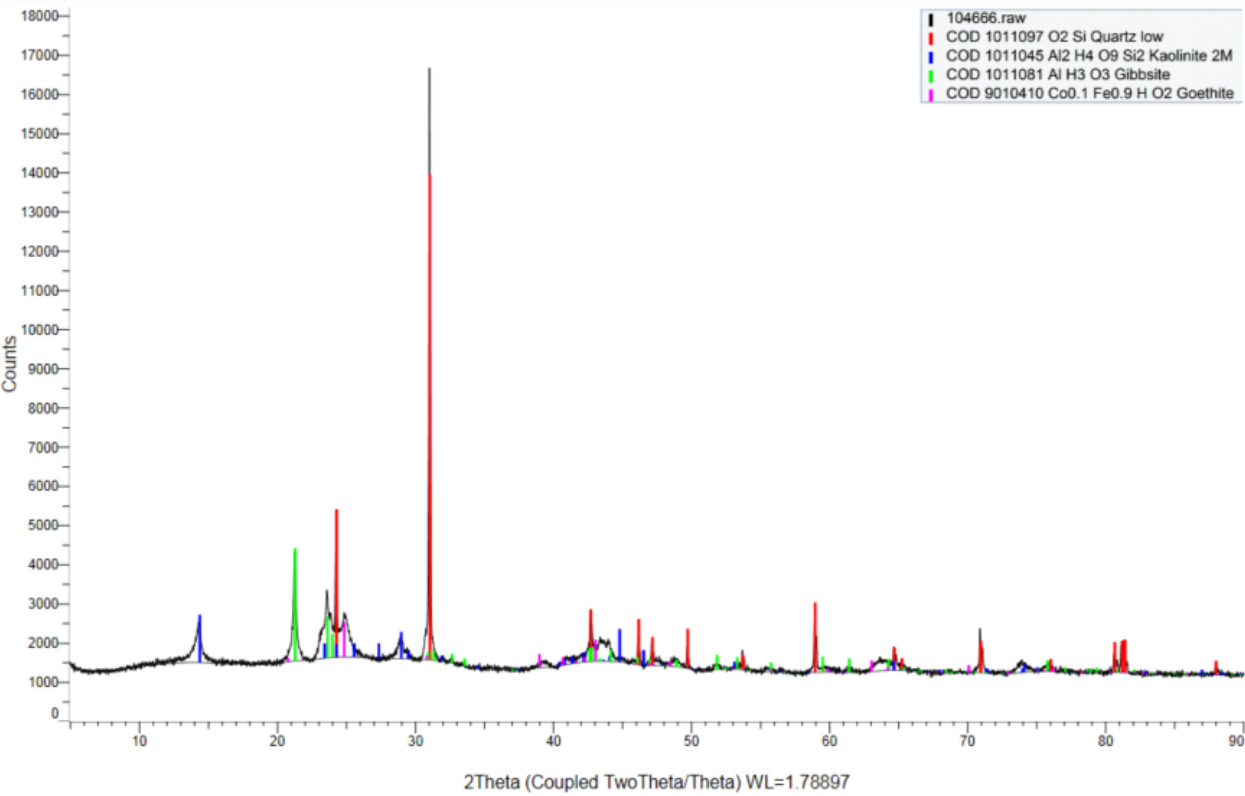


Figure 32. XRD spectra with goethite as the main iron phase.

104658 (Coupled TwoTheta/Theta)

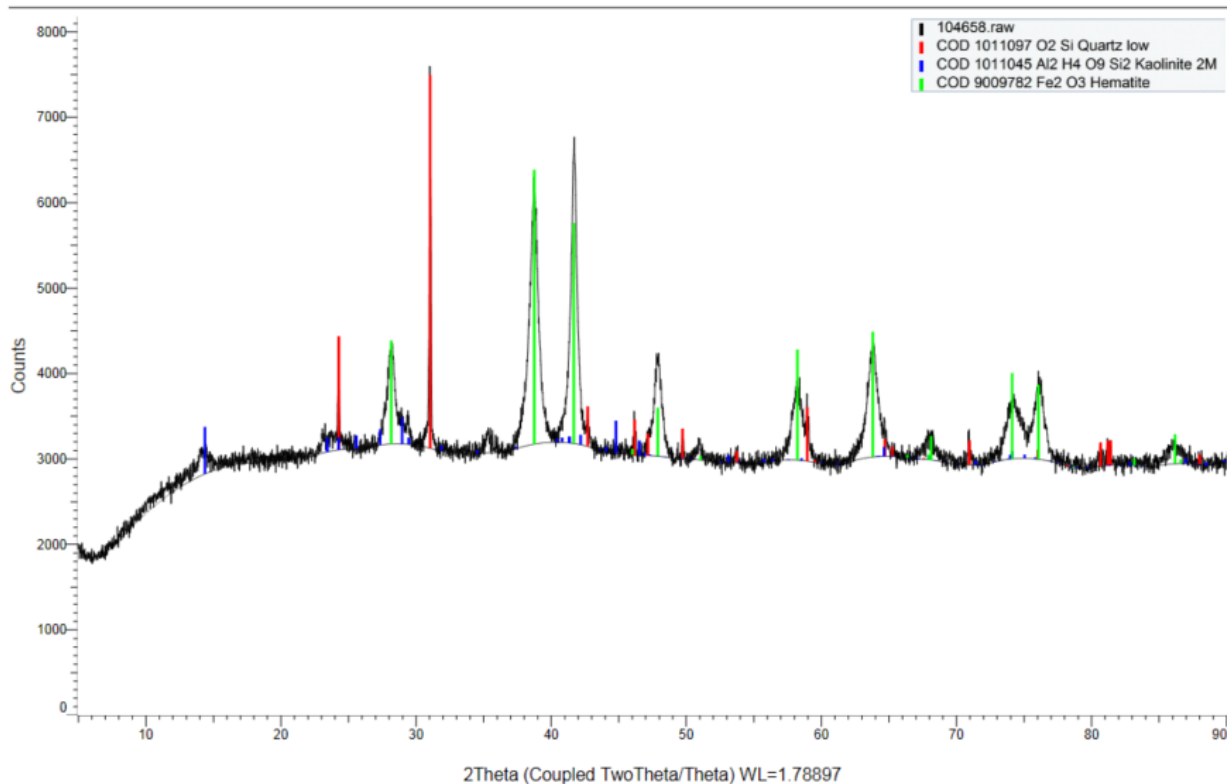


Figure 33 XRD spectra with hematite as the main iron phase.

103738 (Coupled TwoTheta/Theta)

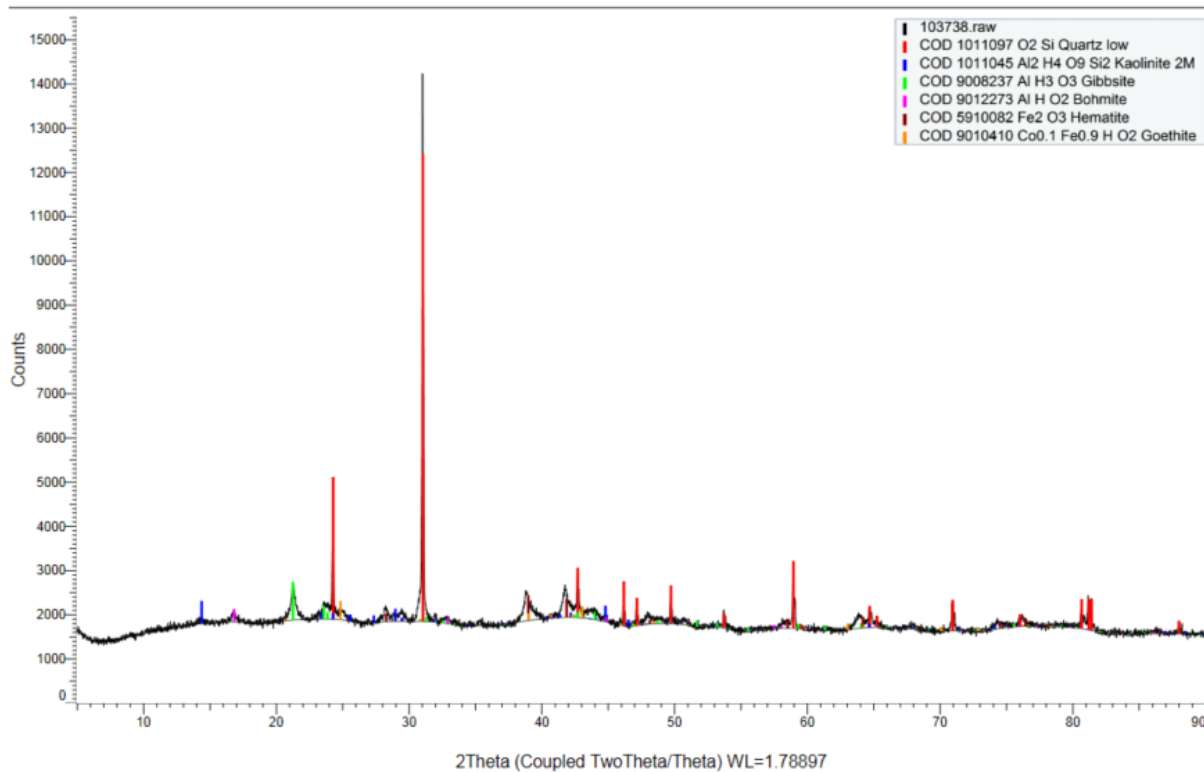


Figure 34. XRD spectra with all aluminium phases present, kaolinite, gibbsite, boehmite.

3.2.3 Scanning Electron Microscopy

The bright-phase mapping was used to identify phases that could potentially be used for further indicator mineral work such as zircon, monazite, tourmaline (schorl) and xenotime (Figure 35). Zircon was the most common of these phases identified, and in one sample copper oxide was detected. The largest proportion among the detected bright-phase minerals are artifacts from the milling process such as chromferide, iron oxides and iron.

Table 3 Quantitative (vol%) results from bright-phase mapping of pulps from 5 laterite samples.

SAMPLE_ID	103652	103505	103801	103726	103650
Quartz	0.00	0.00	0.04	0.04	0.03
Schorl	0.01	0.00	0.18	0.32	0.02
Ferrocapholite	0.00	0.00	0.03	0.02	0.00
Monazite	0.50	0.14	4.19	0.02	0.76
Cuprite	0.00	0.00	0.00	0.00	0.02
Xenotime-(Y)	0.69	0.05	0.03	0.01	1.89
Baddeleyite	0.01	0.04	0.00	0.00	0.18
Baryte	0.00	0.00	0.01	0.00	0.00
Zircon	38.02	6.40	60.43	16.93	52.41
Chromferide	0.29	2.63	3.99	0.37	1.26
Hematite/Magnetite	33.73	29.62	14.06	34.93	17.36
Iron	13.87	54.56	6.88	30.62	13.31
[Unclassified]	12.88	6.54	10.14	16.74	12.74

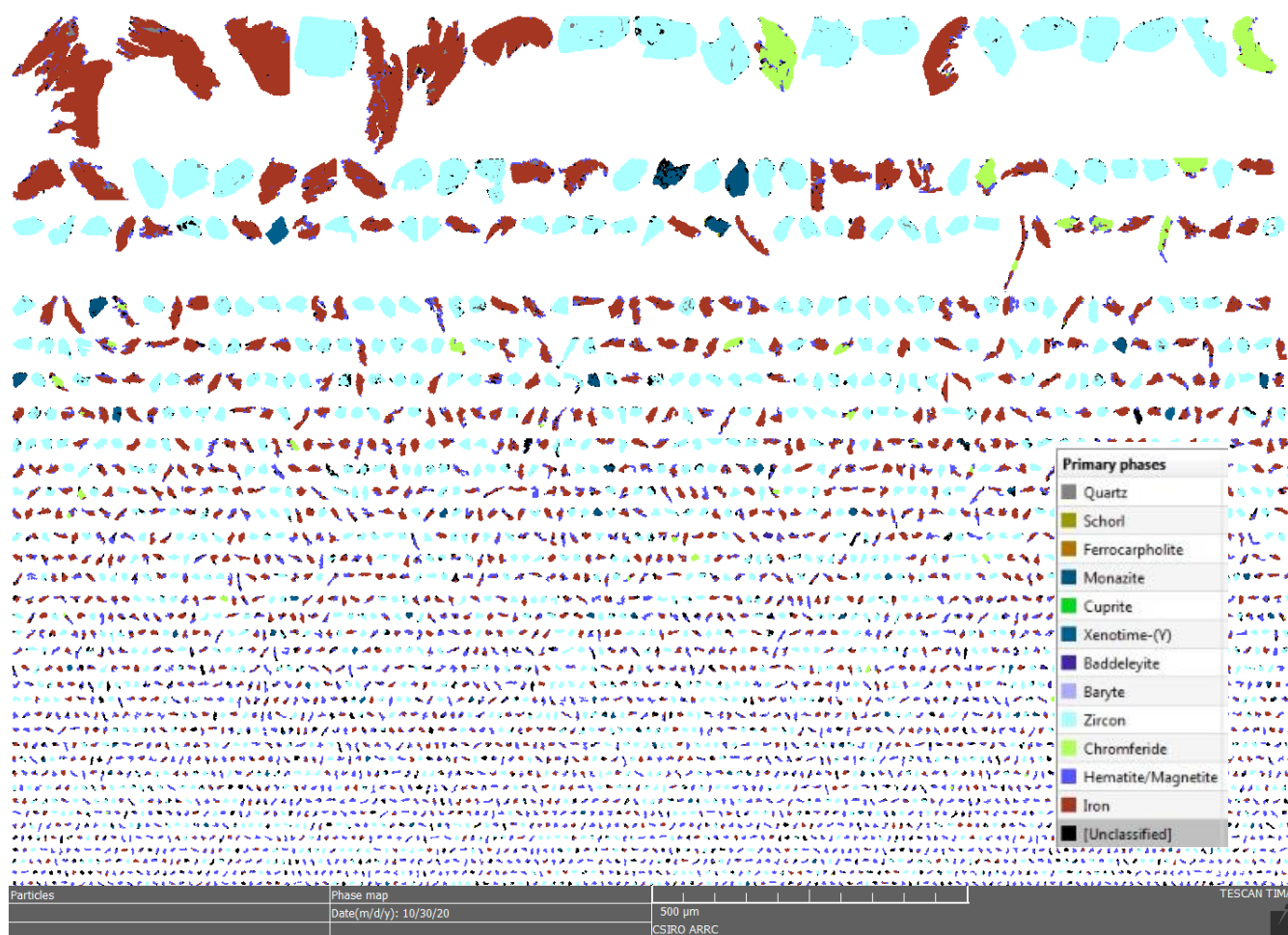


Figure 35 Image of bright-phase mapping particles.

4 Discussion and Future

The project delivered analyses of ~2800 historically collected laterite samples that were held in archive by GSWA and reported by Cornelius et al. (2008). In the earlier assessment several critical elements and Li were not well reported as many of the assays were near limits of detection with the technology available at the time. These project data have improved the detection of these elements making a more useful regional data set for further interpretation. In addition, CSIRO has reported the spectral mineralogy of these samples using the HyLogger-3™ system that was cross validated with XRD and some SEM analysis.

This report outlines an overview of the dataset and presents spatial plots of the new critical metals data that have improved the overall laterite dataset. Further data analysis is recommended as the data are amenable to various data reduction and machine learning approaches, both supervised and unsupervised that were outside the scope of this report.

The initial evaluation of the laterite geochemical dataset for critical metals in the western Yilgarn Craton reveals the following regional patterns:

- In the northeast and central east part of the southwest Yilgarn Craton, the regional sampling shows clusters of elevated Ag around greenstones that is also reflected in Au laterite chemistry and known Au occurrences. These clustered areas are good precious metal target areas for mineralisation. These broad areas are unlikely to have formed just from lateral dispersion of detrital material.
- The regional distribution of Pt shows many yet unexplained and generally untested PGE anomalies throughout a central band in the south western Yilgarn that trends E-W, including the gneissic terrains along the western margin of the craton that extend NE from the recently discovered Julimar deposit. Some elevated Pt values also correspond to areas that showed elevated Au and Ag. Although the new data often present Re as below detection limits, where it is measured, the pattern of Re matches this trend with a few other isolated anomalous results that could be of exploration interest with respect to magmatic Ni mineralisation.
- Elevated Cr indicates the presence of mafic and ultramafic rocks within the Yilgarn and may also highlight areas that host unmapped greenstones in the dominantly granitic rocks of the Yilgarn Craton.
- The new REE data present similar patterns with many elements still at very low concentrations. Overall concentrations indicates that the region has more limited REE exploration potential and/or that the targets and related dispersion are much smaller.
- In contrast the Sn–Ta (pegmatite) signature is greatest in the SW and along the Darling Scarp to the south of Perth and includes the broad Greenbushes area. Other areas of anomalous Sn, Ta, and Nb (and Sb not shown here) may also indicate pegmatites along strike of some greenstone sequences.
- Lithium indicates broad zonation patterns over the western Yilgarn where it highlights areas of evolved magmatic lithologies rather than known lithium deposits themselves (e.g., Greenbushes).

The southern eastern margin is the most enriched Li in the laterite and this correlates with known spodumene $\text{LiAl}(\text{SiO}_3)_2$ that is common in that region.

- Mercury abundances in this data might indicate potential for Au or Ag mineralisation at depth, but these locally associated high Hg results are very isolated (point sources?) without corresponding anomalous Au or Ag at the surface.
- The addition of the HyLogger-3TM spectral data showed major landscape changes in the general mineralogy of the laterite with shifts from a dominance of kaolinite in the NE trending to a dominance of gibbsite in the SW. This variation is related to the intensity of weathering. Gibbsite is formed in well drained areas that receive significant rainfall to leach silica and leave alumina which correspond the known climate changes observed in this area.

The overall data presents valuable new information to mineral explorers in the SW of Western Australia, particularly those that are looking for Li and magmatic Ni-PGEs and to a lesser extent Au. This information is presented as the base results and it is expected that much more could be done with this data set including, but not limited to, machine learning on target types, mineral systems analysis, predictive and uncertainty models and the application or integration of spatial data. The new HyLogger-3TM spectral data will add value to future refinement or ground truthing of spaceborne data and products such as ASTER maps for Fe oxides and kaolinite phases.

5 References

- Berman, M., Bischof, L., Huntington, J., 1999. Algorithms and software for the automated identification of minerals using field spectra or hyperspectral imagery: In Proceedings of the 13th International Conference on Applied Geologic Remote Sensing, Vancouver. Volume 1, pp. 222–232.
- Berman, M., Bischof, L., Lagerstrom, R., Guo, Y., Huntington, J., Mason, P., 2011. An unmixing algorithm based on a large library of shortwave infrared spectra. North Ryde NSW: CSIRO Report EP117468.
- Berman, M., Bischof, L., Lagerstrom, R., Guo, Y., Huntington, J., Mason, P., Green, A., 2017. A Comparison Between Three Sparse Unmixing Algorithms Using a Large Library of Shortwave Infrared Mineral Spectra. March 2017, IEEE Transactions on Geoscience and Remote Sensing, (99) pp.1-23
- Cornelius, M., Robertson, I.D.M., Cornelius, A.J., Morris, P.A., 2007. Laterite geochemical database for the western Yilgarn Craton, Western Australia. Geological Survey of Western Australia, Record 2007/9, 44p.
- Hancock, E.A., Huntington, J.F., 2010. The GSWA NVCL HyLogger: rapid mineralogical analysis for characterizing mineral and petroleum core: Geological Survey of Western Australia, Record 2010/17, 21p.
- Hancock, E.A., Green, A.A., Huntington, J.F., Schodlok, M.C., Whitbourn, L.B., 2013. HyLogger-3: Implications of adding thermal-infrared sensing: Geological Survey of Western Australia, Record 2013/3, 24p.
- Huntington, J.F., Mason, P., Berman, M., 1997. Geological evaluation of The Spectral Assistant (TSA) for mineralogical interpretation: CSIRO, Exploration and Mining Report 417R, 86p.
- Schodlok, M.C., Whitbourn, L., Huntington, J., Mason, P., Green, A., Berman, M., Coward, D., Connor, P., Wright, W., Jolivet, M., Martinez, R., 2016a. HyLogger-3, a visible to shortwave and thermal infrared reflectance spectrometer system for drill core logging: functional description: AJES, vol. 63, no 8, 929–940pp.
- Schodlok M.C., Green, A., Huntington, J., 2016b. A reference library of thermal infrared mineral reflectance spectra for the HyLogger-3 drill core logging system, Australian Journal of Earth Sciences, 63:8, 941-949, DOI: 10.1080/08120099.2016.1234508.

As Australia's national science agency and innovation catalyst, CSIRO is solving the greatest challenges through innovative science and technology.

CSIRO. Unlocking a better future for everyone.

CONTACT US

1300 363 400
+61 3 9545 2176
csiroenquiries@csiro.au

For further information

Ryan Noble
+61 8 6436 8684
ryan.noble@csiro.au
csiro.au/MineralResources

Heta Lampinen
+61 8 6436 8648
heta.lampinen@csiro.au
csiro.au/MineralResources

CRITICAL METALS IN LATERITE RELATED TO PEGMATITE
MINERAL SYSTEMS OF THE WESTERN YILGARN CRATON
(Li, W, Sn, Ta, REE)

A Otto, H Lampinen, T Pinchand, J Huntington and R Noble

A key challenge is to understand the occurrence of critical metals (i.e. Li, Ta, Sn, W, REE) within pegmatite fields, define the fertility of those fields at regional scale, and to discover deposits under cover. This project achieved significant value addition to the 20-year-old collection of ~2800 laterite samples from the southwest Yilgarn Craton. The analytical range has been extended to elements including lithium and platinum. Several elements such as barium, tantalum and tin were reanalysed to achieve much lower detection limits resulting in more precise definition in samples with low abundance. An addition to the dataset are NIR, SWIR and thermal spectral data for most of the samples, collected by the HyLogger-3 system. Overall, the data present valuable new information to mineral explorers in the southwest of Western Australia.



Further details of geoscience products are available from:

First Floor Counter
Department of Mines, Industry Regulation and Safety
100 Plain Street
EAST PERTH WESTERN AUSTRALIA 6004
Phone: +61 8 9222 3459 Email: publications@dmirs.wa.gov.au
www.dmirs.wa.gov.au/GSWApublications